

ROYAL INSTITUTE OF TECHNOLOGY KTH

MASTER THESIS, NANOTECHNOLOGY

DEGREE PROJECT IN APPLIED PHYSICS, SECOND LEVEL

---

# Optical Fibers for Measuring High Voltages

---

*Author:*

**Marcello Graziosi**

881113-5337

graziosi@kth.se

Marcello.Graziosi@acreo.se

*Supervisor:*

**Walter Margulis**

walter.margulis@acreo.se

Acreo Swedish ICT AB

Electrum 236, Stockholm

164 40 , Sweden

**Michael Fokine**

fokine@kth.se

Assistant professor

Laserfysik

4 June 2013

## Abstract

The aim of the degree project is to develop a sensor based on poled optical fiber for measuring voltages in power stations: few hundreds of KiloVolt (kV) at  $50Hz$ . A two-holes fiber is filled with two metal columns of BiSn and thermally poled. Poling parameters are characterized by using a Mach-Zehnder Interferometer (MZI) configuration. The poled fiber can be used as sensing element, because it works as a phase modulator when an electric field is applied through it. Then, a poled fiber is inserted into a Sagnac interferometer to analyze how it responds to pulse voltage and sine wave voltage signals: the applied voltage  $V_{app}(t)$  modulates the interference between clockwise(CWS) and counterclockwise(CCWS) light.

Afterwards the setup is modified to be suitable for voltage measurements in power stations. The Sagnac loop is made longer, a lock-in amplifier is used for filtering the output, a longer poled fiber is inserted in the loop and it is sandwiched between two electrostatic plates to measure an electric field generated externally the fiber: no contact is made with the internal fiber electrodes, indeed they have been removed in one component. A  $50Hz$  sine wave signal with voltage peak to peak  $V_{pp}$  of  $170V$  is measured by using the parallel plates configuration with a  $0.750mm$  distance: electric field of  $0.23MV/m$ . Higher sensitivity is achieved at higher frequencies: electric field of  $100V/m$  is clearly detected at a frequency  $1.35kHz$ .

# Contents

<b>1</b>	<b>Introduction</b>	<b>3</b>
1.1	Aim and motivation of the project . . . . .	3
1.2	Outline of the thesis . . . . .	3
<b>2</b>	<b>Theory</b>	<b>5</b>
2.1	Poling of fibers . . . . .	5
2.2	Sagnac interferometer . . . . .	6
<b>3</b>	<b>Poling process and characterization</b>	<b>8</b>
3.1	Experimental procedure . . . . .	8
3.1.1	Filling the fiber . . . . .	8
3.1.2	Shifting the electrodes . . . . .	11
3.1.3	Preparation for poling . . . . .	12
3.1.4	Poling . . . . .	15
3.2	Characterization and data analysis . . . . .	16
<b>4</b>	<b>Measurements with Sagnac interferometer</b>	<b>19</b>
4.1	Set up . . . . .	19
4.2	Short electrical pulse . . . . .	20
4.3	Malus law . . . . .	21
4.4	Sinusoidal voltage . . . . .	22
4.5	Intensity detected in a Sagnac . . . . .	25
<b>5</b>	<b>Sagnac interferometer and poled fiber for 50Hz electric field measurements</b>	<b>30</b>
5.1	Lock-in amplifier and longer loop . . . . .	31
5.2	Longer poled fiber . . . . .	32
<b>6</b>	<b>Contactless detection of electric field</b>	<b>37</b>
6.1	Measurements of an electric field generated externally the fiber .	37
6.2	Mobile plate . . . . .	41
<b>7</b>	<b>Low fiber with a low coherence interferometer</b>	<b>42</b>
<b>8</b>	<b>Conclusion</b>	<b>44</b>
<b>A</b>	<b>Appendix</b>	<b>45</b>

# 1 Introduction

## 1.1 Aim and motivation of the project

The electricity that we have in our homes is a voltage signal of 220V rms with a frequency of 50Hz, but its amplitude is much higher at the beginning of the transmission line (it might be nearly 1MV), where it is produced and transmitted by the power stations. Measuring such a high voltage is an issue: large capacitor banks are currently used to divide and reduce the signal, before it can be measured. These sensors are bulky and expensive, fig.1. In contrast a sensor



*Figure 1: Capacitor bank and power transformer to step high voltage down to a safe level.*

based on optical fiber is cheaper, it has a much simpler structure and it can be implemented in an optical line, in such a way that a network can be built to have a single station from which the voltage is monitored at several different positions of the transmission line. A High Voltage (HV) optical sensor working at 50Hz has already been presented few years ago: it is based on a birefringent thermally poled fiber and the modulation of the light is measured by using a low coherence interferometer[1] [2]. In this experimental thesis an alternative HV optical sensor is studied: non-symmetric two-holes silica fibers are poled and used as sensing element in a Sagnac interferometer. Poled fibers show a Linear Electro-Optical (LEO) property: an applied electric field through the fiber changes the refractive index of the guided light according to a linear relation. As a consequence the light phase is shifted and therefore a phase modulation of the light can be achieved by applying AC voltage through the poled fiber. To detect and measure the phase modulation, a Sagnac interferometer is used, where the poled fiber works as phase modulator in the Sagnac loop.

## 1.2 Outline of the thesis

The project can be divided in three parts: procedure for poling fibers, measurements with a Sagnac interferometer and detection of 50Hz AC voltage with a Sagnac interferometer. First the poling process is studied and performed. The

fiber requires a long and delicate preparation, after which it is thermally poled by using hot plate and high voltage applied through metal electrodes that are placed inside the fiber. Afterwards the poling parameter are characterized and the value of the 2nd order non-linear coefficient  $\chi^{(2)}$  is calculated. In the second part, a Sagnac interferometer is built with a poled fiber in the loop, which works as phase modulator when a voltage signal is applied. The light interference is detected and studied for applied voltage in the form of short-pulses and then in the form of sine-waves: several sets of measurements are taken by varying parameter of the voltage signal as frequency and amplitude. To satisfy the requirement of the project, the developed sensor should detect a minimum electric field of at least 5kV/m at 50Hz, however this type of signal could not be detected in this part of the project: both the frequency and the amplitude are too low. In the third part, improvements are made to the Sagnac interferometer and a 50Hz voltage signal is detected. Three poled fibers components are fabricated and two parallel metal plates are used to sandwich the components and apply an electric field externally to the fiber. By applying a potential difference between the electrodes inside the fiber, a voltage signal of 30V 50Hz is detected. Then, when the potential difference is applied between the parallel plates, a 200V 50Hz signal is detected: contactless detection. In one component the internal electrodes are successfully removed after poling. This component is then successfully used to detect a potential difference applied across the parallel plates. In the end, a briefly description of a different type of optical sensor for HV is presented and it is discussed which future improvements can be made to the sensor realized in this diploma work.

## 2 Theory

### 2.1 Poling of fibers

When an external electric field  $E_{ext}$  is applied to a silica fiber, its refractive index varies according to the Kerr effect:

$$\Delta n = \frac{3\chi^{(3)}}{2n_0} E_{ext}^2 \quad (1)$$

where  $n_0$  is the average refractive index of the fiber and  $\chi^{(3)}$  is the 3rd order susceptibility of silica [3][4]. A refractive index variation brings to a change of the phase  $\phi$  of the light travelling through the material:

$$\Delta\phi = \frac{2\pi L\Delta n}{\lambda} \quad (2)$$

where  $L$  is the length of the region and  $\lambda$  is the wavelength inside the region that does not experience  $E_{ext}$ ; therefore the function  $\Delta\phi$  vs.  $E_{ext}$  is a parabola with the vertex in  $(0,0)$ , blue parabola in fig. 2. However, the process of poling

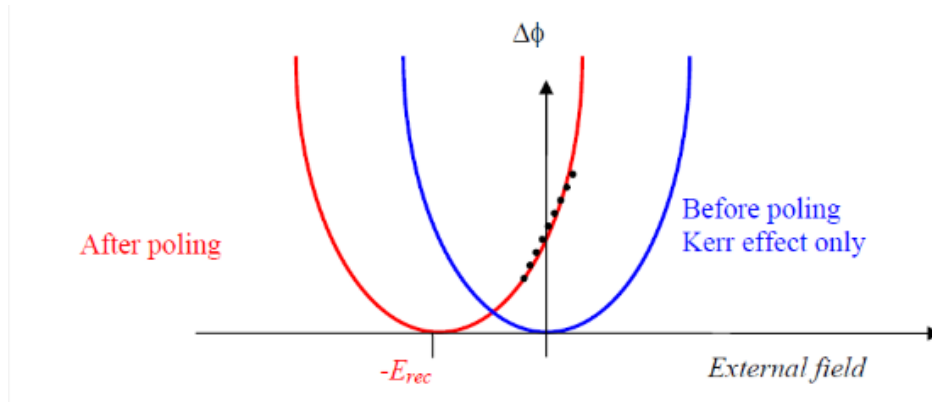


Figure 2:  $\Delta\phi$  vs.  $E_{ext}$  is a parabola that can be shifted by poling process. The black dots show that a linear approximation can be done when  $E_{ext}$  is limited in a range around zero [4].

induces a permanent electric field (recorded electric field)  $E_{rec}$  inside the fiber, that results in a shift of the  $\Delta\phi$  vs.  $E_{ext}$  parabola: the vertex shifts to the new position  $(-E_{rec}, 0)$ , red curve in fig. 2. If the shift is large enough, then a little modulation of  $E_{ext}$  around the zero gives a change of  $\Delta\phi$  that can be approximated as linear: linear electro-optical (LEO) effect.  $E_{rec}$  adds to  $E_{ext}$  in eq.1, then the change in refractive index becomes:

$$\Delta n = \frac{3\chi^{(3)}}{2n_0} (E_{ext} + E_{rec})^2 = \frac{1}{2n_0} (3\chi^{(3)} E_{ext}^2 + 6\chi^{(3)} E_{ext} E_{rec} + 3\chi^{(3)} E_{rec}^2) \quad (3)$$

Eq.3 describes the shifted Kerr parabola, red curve in fig.2. An effective 2nd order non-linearity coefficient is defined as:

$$\chi_{eff}^{(2)} \stackrel{def}{=} 3E_{rec}\chi^{(3)} \quad (4)$$

then, when  $E_{ext} \ll E_{rec}$ , eq.3 can be approximated to:

$$\Delta n = \frac{1}{2n_0} (2\chi_{eff}^{(2)} E_{ext} + 3\chi^{(3)} E_{rec}^2) \quad (5)$$

where  $\Delta n$  depends linearly on  $E_{ext}$  [3] [4].

The basic idea behind the poling process is that in a silica fiber there are small concentrations of impurities as 1ppm of sodium (Na) ions. If the ions are moved and relocated in an anisotropic way, then the charge distribution inside the fiber is rearranged and an electric field  $E_{rec}$  can be recorded. The process is done in three main steps:

- the fiber is heated up to increase the ions mobility
- an electric field is applied across the fiber to move and relocate the ions
- the fiber cools down while the applied electric field is still on: in this way the ions are frozen into new positions

A quantitative evaluation of the poling process is given by the 2nd order non-linearity coefficient  $\chi^{(2)}$  (or Pockels coefficient) that is measured in picometer over Volt (pm/V): the larger the better. Before poling the value of  $\chi^{(2)}$  in silica is zero, but there are nonlinear materials that have already an intrinsic second-order nonlinearity, for instance lithium niobate ( $LiNbO_3$ ) has  $\chi_{LiNbO_3}^{(2)} = 30.9 \text{ pm/V}$ . After poling, silica fibers show a non-zero  $\chi^{(2)}$  (or  $\chi_{eff}^{(2)}$ ), that typically has a value of  $\chi^{(2)} \sim 0.2 \text{ pm/V}$  [2].

As already discussed, the phase modulation in a poled fiber is generated by an electric field, however it is common to refer to the applied voltage, that is linearly proportional to the generated electric field. An important poling parameter is the so-called  $V_\pi$ , that is the applied voltage needed to generate an electric field that gives a phase shift of  $\Delta\phi = \pi \text{ rad}$ .

## 2.2 Sagnac interferometer

An interferometer is a very suitable configuration to detect a phenomenon that modulates the phase of light. The basic idea is that a light beam is divided in two beams that travel along two different paths. The two beams undergo to a different phase modulation and, when they recombine, they have two ways out: depending on the difference in phase, the intensity of the light is split between the two output. Fig. 3 shows the three more common types of interferometer: Sagnac interferometer, Michelson interferometer(MI) and Mach-Zehnder Interferometer (MZI).

In a MI the light is split in two arms(two guiding fibers) and the phase is modulated only along one arm. Then the light is reflected back in both arms and the two light beams interfere each other: depending on the relative phase shift the light goes either to the detector or back to the laser. In a MZI the light is not reflected back, but it couples after having been guided by the two arms and then it is detected. In a Sagnac interferometer a coupler splits the light inside a closed loop, one light beam travels clockwise and the other one counterclockwise. Both the light beams experience a phase modulation, but the

Sagnac loop creates a delay between the two beams: if the clockwise light is modulated at the time  $t$ , then the counterclockwise light is modulated at the time  $t + \Delta t$  where  $\Delta t$  is the delay given by the loop. Therefore, the interference depends on how the phase modulation changes after the time  $\Delta t$ . However, if the phase modulation is placed in the center of the loop, then there is no delay, thus there is no modulation of the interference. A poled fiber can be used

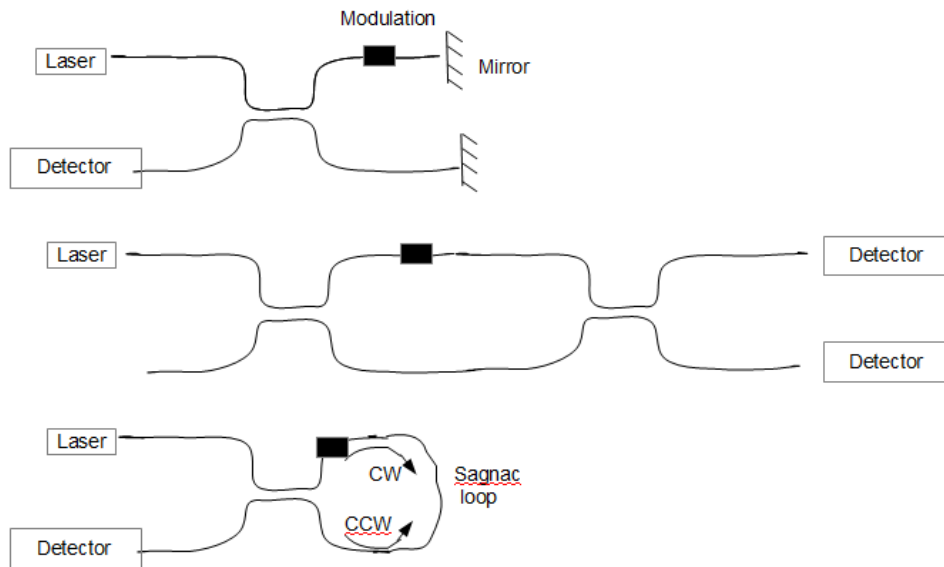


Figure 3: Three interferometer: a MZI can be seen as two MIs, where the light is not reflected but it goes into a second coupler and then the two outputs are detected. In a Sagnac loop the phase modulation can be given for instance by rotating the system: a clockwise rotation results in a longer path for the light beam that travels clockwise.

as phase modulator by exploiting its LEO property: if one applies a voltage that gives a phase shift of  $\pi$  rad, then the interference goes from destructive to constructive, that means all the light switches from one exit of the interferometer to the other exit. The main advantage of the Sagnac interferometer is that both the beams travel in the same fiber. The polarization of the guided light is very sensitive to even very small thermal fluctuations and mechanical stress. This means that in a MZI and in a MI, if one arm of the interferometer experiences a random polarization change, for instance a small temperature variation, that is not felt by the other arm, the detected interference might be largely affected and one can not distinguish the phase shift given by the desired modulation (applied voltage) from the phase shift given by uncontrolled random variations as thermal fluctuations or mechanical stress. On the contrary, in a Sagnac loop the two beams travel along the same path within a very short delay (the speed of light in a Silica fiber is  $2 \cdot 10^8$  m/s), therefore the uncontrolled random variations given by the environment are nearly the same for both of them and do not affect the output signal.



### 3 Poling process and characterization

#### 3.1 Experimental procedure

The employed optical fibers are non-symmetric two-holes silica fibers with a cladding of pure silica where the impurity level is nearly 1ppm of Sodium (Na) and the refractive index is  $n_{clad}=1.460$  for light wavelength of  $\lambda = 1.55\mu m$ . The core is Germanium-doped Silica(97% silica and 3% Ge) with  $n_{core}=1.465$  for  $\lambda = 1.55\mu m$ . The total diameter of the fiber is  $125\mu m$  plus the acrylic coating. Metal electrodes consisting of 58Bi42Sn (58% Bismuth and 42% Tin) are inserted into the two-holes fiber, fig.4.



Figure 4: a) Front of a non-symmetric two-holes fiber [4]. b) The holes have a diameter of  $27\mu m$  and a distance of  $22.7\mu m$ . BiSn is seen inside the holes.

The poling process can be divided in four stages: "filling the fiber", "shifting the electrodes", "preparation for poling" and "poling".

##### 3.1.1 Filling the fiber

The first stage takes nearly two hours. The basic idea is to push liquid metal inside the fiber by applying high pressure, [5]:

- 58Bi42Sn is melted inside an oven at  $160^{\circ}C$ . The metal is in a small container that is sealed and pressurized.
- few two-holes fibers are squeezed in a gasket and inserted in a screw that is turned in the lid of the metal container, fig.5.
- few centimeters of fibers must come out of the gasket: this part is going to sink into the liquid metal. Here the acrylic coating is removed and few millimeters of fiber are cut. This process aims to prevent that some small piece of acrylic or glass goes inside the holes: if the holes are blocked, the metal will not go inside the fiber.
- when the metal is liquid, the lid is screwed on the container: in this way the fibers are dunked and the container is pressurized.
- the entire assembly, fig.5, is placed into the oven. When the temperature is  $160^{\circ}C$ , nitrogen gas at 3.5atm is sent into the sealed container and BiSn is forced up into the fiber, fig.6.

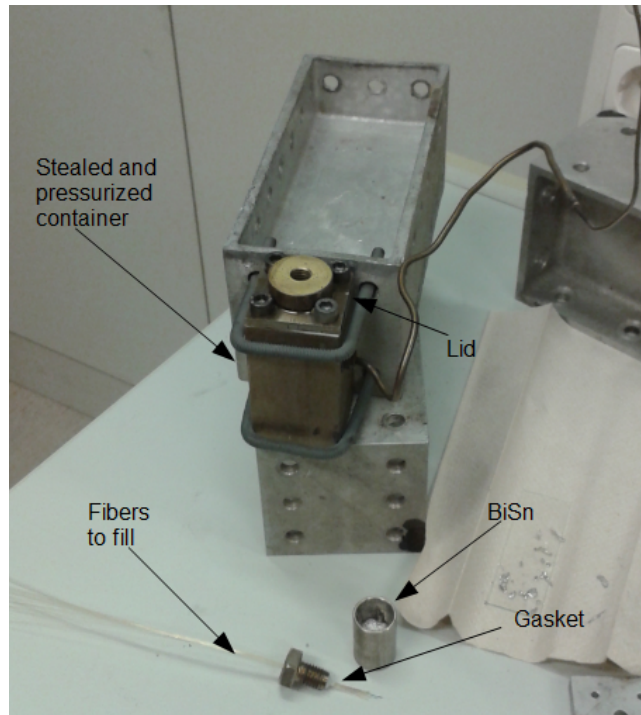


Figure 5: Setup used for filling the fiber: the fibers are squeezed in the gasket, then they are screwed in the lid of the sealed container.

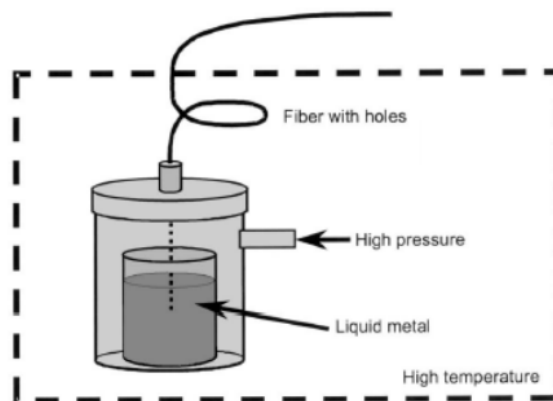
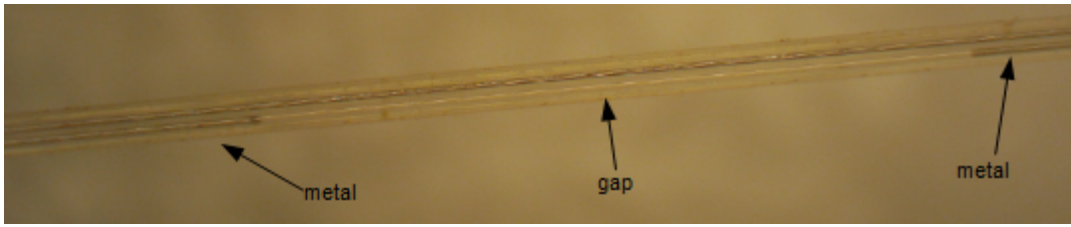


Figure 6: Schematic diagram of the technique for filling the fibers with metal [5].

- 12cm of fiber are left outside the oven: BiSn goes up only into the part of fibers that is inside the oven, then it solidifies and it stops going up. Few empty centimeters of fiber are necessary to be able to splice the two-holes fiber with a standard fiber.
- for 20 min. the oven temperature is kept to 160°C and the pressure to 3.5atm, then the oven is turned off and it slowly cools down.
- when the temperature is about 90°C (after nearly 50min.), the pressure is turned off and the fiber are removed from oven.
- the fibers are blocked in solid BiSn, therefore they are cut and analyzed under a microscope to check that the electrodes are continuous.

When the working fiber is long (more than 1m), unluckily it often happens that the electrodes are not continuous, but there are gaps, as shown in fig.7. The gap breaks the electrical connection, therefore the fiber needs to be emptied from the metal and filled again.



*Figure 7: A gap is formed in one electrode after the stage of "filling".*

### 3.1.2 Shifting the electrodes

If there are no gaps, the next stage is "shifting the electrodes". When the poling process will be completed, the two-holes fiber will be spliced with standard fibers, however it is not possible to splice the fibers if there is metal up to the end of the fiber. On the top of the filled fibers, there are roughly 12cm that were left empty. On the contrary, where the fiber was sunk into the metal, BiSn goes up to the end of the fiber. For this reason the electrodes need to be shifted. "Shifting the electrodes" takes around 1h 30min.:

- BiSn is removed from the container of fig.5.
- As it was done in the "filling" stage, acrylic coating is removed at the end of the fiber and few millimeter are cut to prevent that particle might block the holes.
- the lid is screwed and the end of the fibers is inside the sealed container, but this time there is not melted BiSn.
- only 7cm are left outside the oven, then the temperature is brought to 160°C and 3.5atm are applied.
- After 30min. the oven is switched off and it slowly cools down to 90°C . Then the pressure is turned off and the fibers are ready for being processed for the poling. Fig.8 shows the shifting of the electrodes.



*Figure 8: After the second stage, there are 7cm of empty holes on one end of the fiber and 5cm of empty holes on the other end.*

### 3.1.3 Preparation for poling

A standard fiber (without holes) is spliced to the end of the two holes fiber that has 5cm of empty holes. To splice two fibers, first the acrylic coating has to be removed for few centimeters from both the fibers, fig.9, then the fiber is cleaved: in this way the two surfaces that are joined are clean and flat. If one surface is tilted, then the splicing region will give a big loss. The most

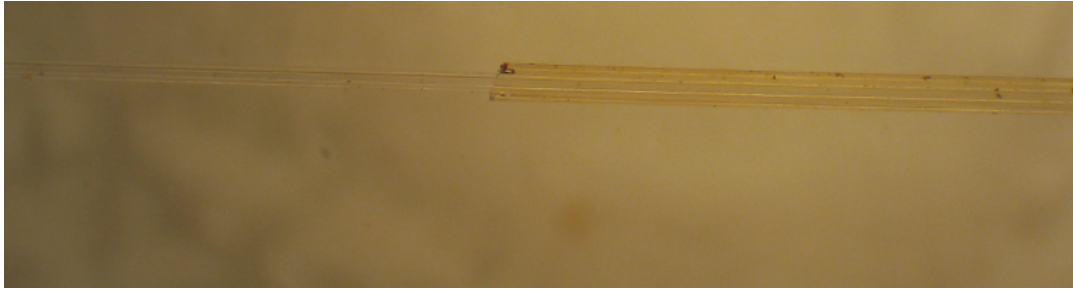


*Figure 9: On the left the acrylic coating was removed and here the fiber looks thinner: the diameter goes from  $210\mu\text{m}$  to  $125\mu\text{m}$ .*

straight forward way to remove the acrylic coating is to take pliers and strip the coating. However in some cases the coating might be harder than usual, then the fiber is sunk into dichloromethane for 30sec., after that the coating is easily stripped away. The poling process occurs at  $265^\circ\text{C}$ , this temperature is enough high to burn the acrylic and make it so hard that neither the dichloromethane will help in remove it. Therefore, in case burned acrylic coating needs to be stripped away, hot sulfuric acid  $\text{H}_2\text{SO}_4$  is used, fig.10. The acid is heated up to  $\sim 110^\circ\text{C}$ , then the fiber is sunk into it for few minutes. After that the fiber is delicately moved in water for removing the burned coating. To make the

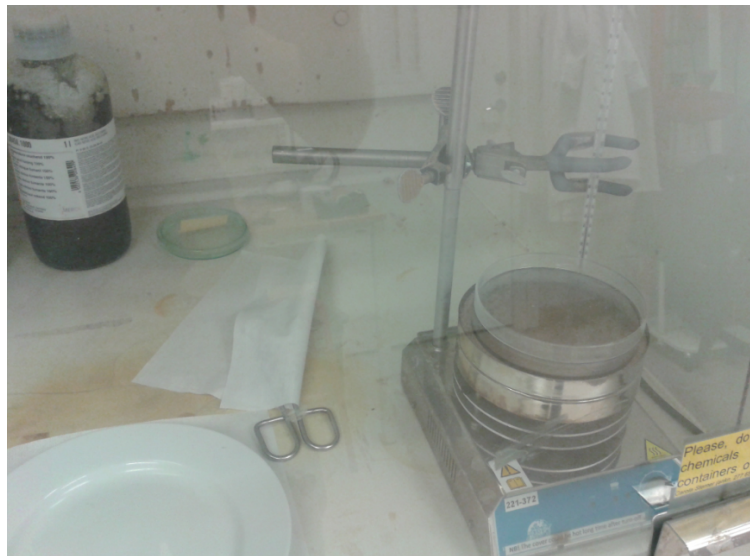


*Figure 10: The process of removing coating with sulfuric acid is done in a chemical lab. Sulfuric acid has to be kept under a hood.*

electrical connection needed for poling, the fiber is polished to expose both the electrodes to the outside, fig.11. A soldering iron locally melts the BiSn and



Figure 11: Coating and part of the cladding are removed. Here the fiber is very fragile.

gold coated tungsten wires are connected with the electrodes, fig.12. Then the fiber is turned of 180°C and polishing is repeated to expose the other electrode. The fiber has to be handled very carefully, because it is very fragile in all the

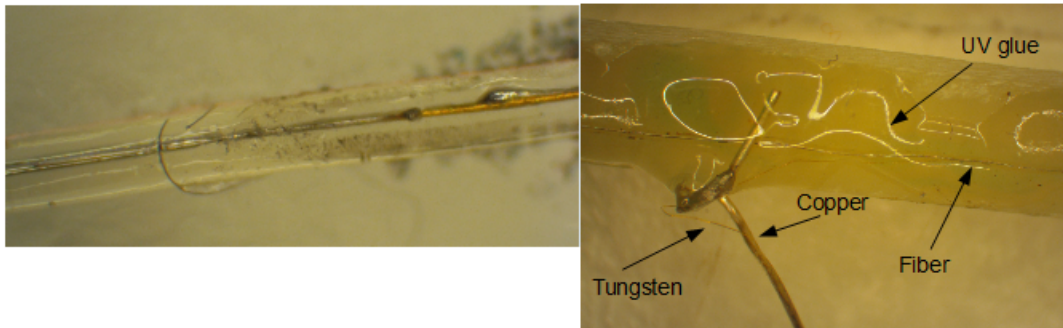


Figure 12: On the left gold coated tungsten wire (yellow wire) is connected with the BiSn electrode: the gray drop is BiSn that was moved when the W wire was inserted. On the right UV glue is used to stick the fiber on the plastic frame. Attention has to be paid for not glue the entire tungsten wire. Afterwards, a connection is done between copper and tungsten wire by dropping melted metal on them.

three regions where the acrylic coating was removed: the two polished regions for the W wires connections and the splicing region between the two-holes and the regular fiber. Subsequently a plastic frame is glued to the region of the connections, fig. 12. There are two main reason for do this: first the polishing regions are more protected, second copper wire can be connected to the W wires. Copper wire are much thicker and easier to connect with a voltage generator. Moreover tungsten has a poor conductivity, thus it is better to have W wires as short as possible.

For the poling process the two W wire connections are on both the electrodes; but if the connections are on the same electrode, then a multimeter can be used to measure the resistance  $R$  across the BiSn electrode and its resistivity  $\rho$  can be calculated. A resistance of  $R = 131.8\Omega$  is measured for a length of  $l = 1cm$ . Since the diameter of the electrode is the hole diameter  $d = 27\mu m$ , the cross section area is  $A = (d/2)^2\pi = 572.56\mu m^2$ . Then, the resulting resistivity is:

$$\rho = \frac{A \cdot R}{l} = 7.546 \cdot 10^{-6} \Omega m$$

Since the poling process is performed at  $265^{\circ}\text{C}$ , the electrodes will be melted inside the fiber holes; to avoid BiSn to move along the fiber and eventually form air gaps, a syringe needle is glued on the free end of the two-holes fiber: a syringe is used to apply a pressure inside the fiber holes, in such a way that the melted BiSn is held together. Fig.13 shows what happens to the electrodes when they are heated above the melting temperature if no pressure is applied to hold the melted metal together.

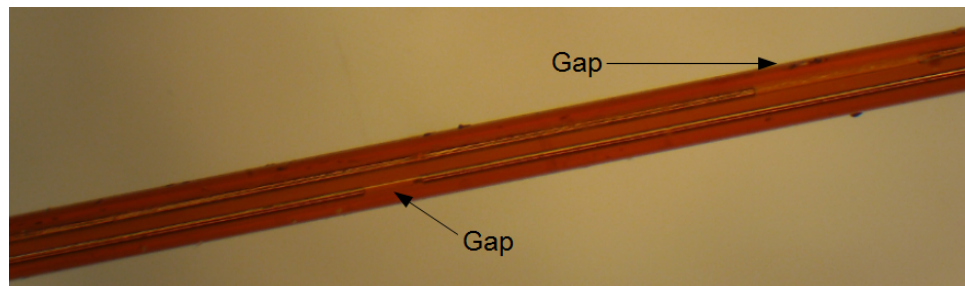


*Figure 13: Above the BiSn melting temperature of  $138^{\circ}\text{C}$ , the electrodes melt and moves inside the hole. Consequently gaps are formed.*

### 3.1.4 Poling

The fiber is placed on a hot plate that is grounded, fig.14. a positive voltage of +4kV is applied on both the electrodes and the hot plate is quickly heated up to 265°C . After 3h 15min the hot plate is turned off and it slowly cools down,

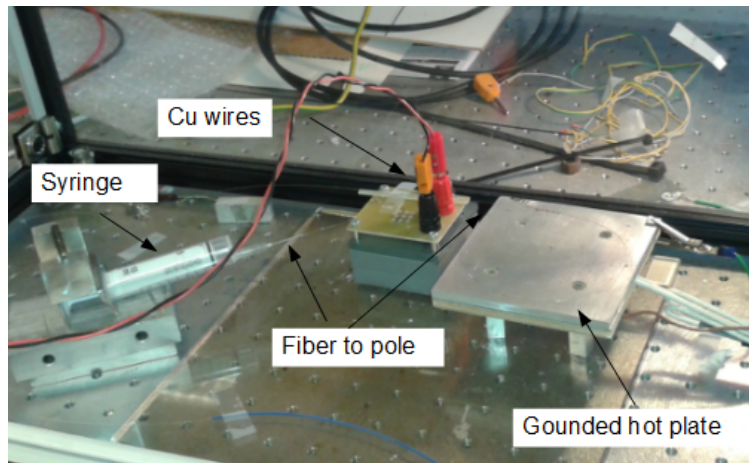


Figure 14: Picture of the set up used for poling: fiber is connected to a voltage generator by copper wires and it is placed on a grounded hot plate.

when the temperature is below  $< 100^{\circ}\text{C}$  the voltage is switched off: the charged particles can be considered as frozen (stuck) in their new position, where they give rise to the recorded electric field  $E_{rec}$  across the fiber. Since the etching rate of fibers depends on the concentration of impurities, one can see the relocation of the ions by etching the fiber in Hydrofluoric acid (HF). As fig. 15 shows, a depletion region is formed around the electrodes. Since the holes diameter is  $27\mu\text{m}$ , one can estimate that the ring of the depletion region has a width of nearly  $10\mu\text{m}$ .

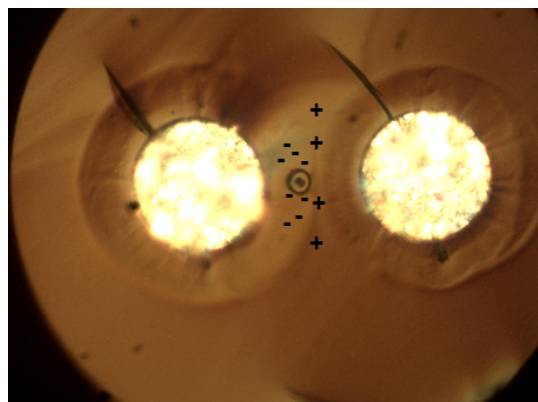


Figure 15: A poled fiber was etched in HF for 50s. The shiny parts are the two metal electrodes, around them the etching is slower because the ions are moved away during poling. Between the two rings there is an accumulation of positive ions, whereas the core is inside a depletion region, that is a negatively charged.



### 3.2 Characterization and data analysis

After poling, the component (the poled fiber) needs to be handled very carefully, because the coating is burned and this makes the fiber more fragile. Due to the high temperature, the acrylic shrinks, becomes harder and its colour becomes dark brown, therefore the internal electrodes can not be seen in a clear way. Moreover, after poling the coating breaks in several points, making the component even more fragile, fig.16. To characterize the poling parameters, the

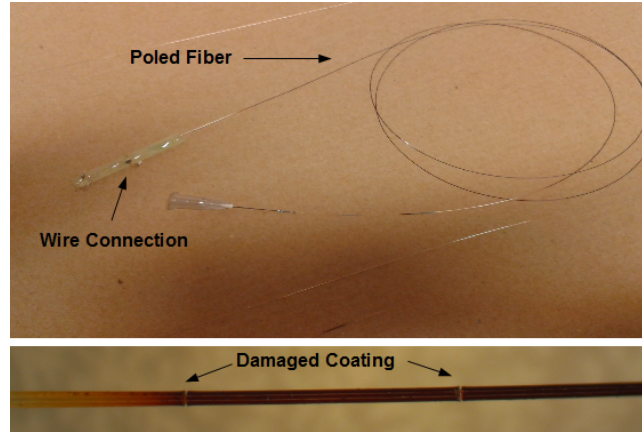


Figure 16: On the top, a fiber after poling. On the bottom the acrylic coating is burned and broken in two points. After 3h 15min at 265°C, the fiber diameter (cladding and coating) shrinks from 210 $\mu\text{m}$  to 175 $\mu\text{m}$ .

fiber is spliced to two connectors and a MZI is used, fig. 17: the poled fiber is placed along one arm of the MZI and a potential difference of triangular shape with frequency  $\nu = 24\text{Hz}$  is applied through the fibers electrodes.

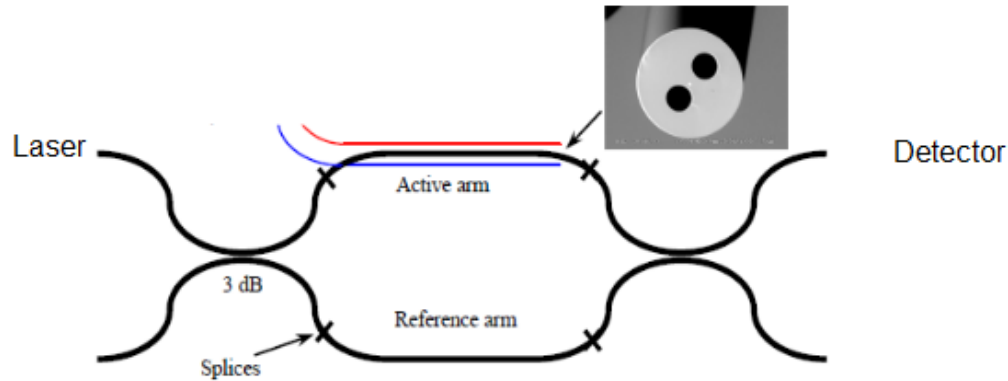


Figure 17: MZI configuration used for characterizing the poled fiber: a triangular voltage is applied to the poled fiber [4].

The applied potential difference  $\Delta V$  ranges between 0-2.3kV and corresponds to an external electric field  $E_{ext} = \Delta V/d$ , where  $d = 22.7\mu\text{m}$  is the electrodes distance. Each time that  $E_{ext}$  gives a phase shift  $\Delta\phi$  that is a multiple of  $\pi$ , the interference is switched from constructive to destructive, as shown in fig. 18.

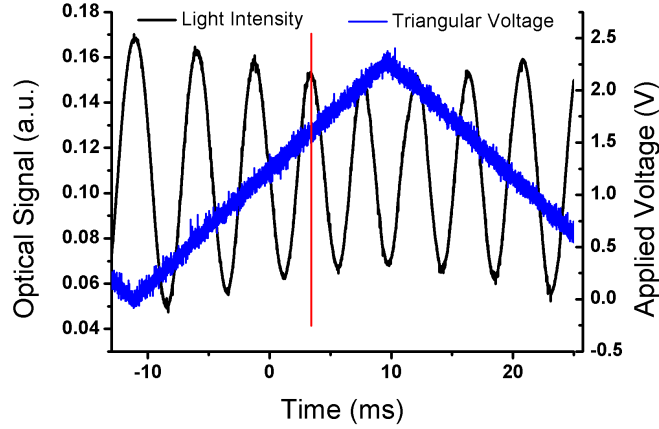


Figure 18: Results of the characterization: the data are recorded by using an oscilloscope. The red line is used to see the value of voltage (blue line) that corresponds to each peak or trough of the light intensity.

From fig.18 one can read the values of the applied voltage (blue curve) that corresponds to all the peaks and troughs: the first peak sets the zero, then there is the first  $\pi$  shift ( $V_\pi$ ), then the second and so on. After that, the positive and negative electrodes are inverted. In this way the peaks and troughs corresponds to phase shifts that are multiples of  $-\pi$ . The data are plotted in fig.19. According to eq.2 and eq.3, a parabolic curve ( $ax^2 + bx + c$ ) is used

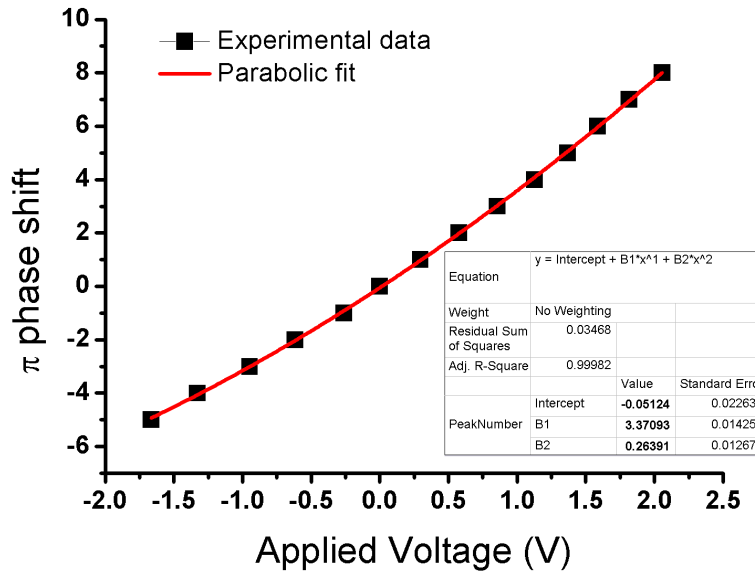


Figure 19: Parabolic fit: the voltage ranges within  $\pm 2.3kV$  and there are 8 positive and 5 negative  $\pi$  shift. The fit parameters are:  $a = 0.264kV^{-2}$ ,  $b = 3.37kV^{-1}$ ,  $c = -0.051$ .

to fit the data and the fitted parameters are shown in the insert of fig.19. To calculate the value of the second order non-linear coefficient  $\chi^{(2)}$  we use the following parameters:  $\lambda = 974nm$ , electrodes distance  $d = 22.7\mu m$ , refractive

index  $n = 1.48$  and poled length  $l = 20\text{cm}$ . Then the calculations are the followings:

- recorded voltage :  $V_{rec} = \frac{b}{2a} = 6.48\text{kV}$
- recorded electric field :  $E_{rec} = \frac{V_{rec}}{d} = 2.855 \cdot 10^8 \frac{\text{V}}{\text{m}}$
- 3rd order susceptibility :  $\chi^{(3)} = \frac{a \cdot \lambda \cdot d^2 \cdot n}{3l} = 3.057 \cdot 10^{-22} \frac{\text{m}^2}{\text{V}^2}$
- 2nd order non-linearity( or  $\chi_{eff}^{(2)}$  ) :  $\chi^{(2)} = 3 \cdot E_{rec} \cdot \chi^{(3)} = 0.262 \cdot 10^{-12} \frac{\text{m}}{\text{V}} = 0.262 \frac{\text{pm}}{\text{V}}$

## 4 Measurements with Sagnac interferometer

### 4.1 Set up

A poled fiber is used to modulate the phase of light in a Sagnac loop configuration as in fig.20 : the source is a  $\lambda = 1.55\mu m$  laser with emission power of  $-0.74dB$ . A 3dB coupler splits the light 50-50 into the two entrances of the

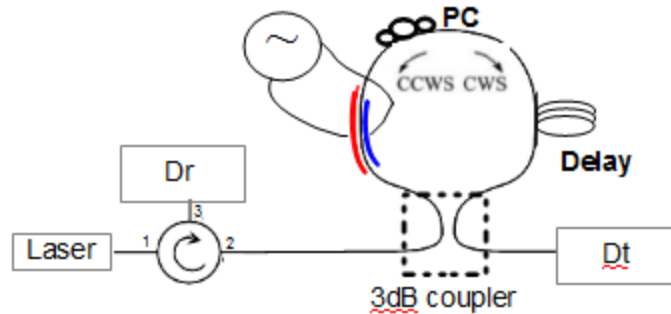


Figure 20: Sagnac interferometer:  $Dt$  and  $Dr$  are the detectors for transmitted and reflected light, a mickey mouse Polarizer Controller (PC) and a component are inserted in the loop. A voltage generator is connected to the electrodes inside the poled fiber. A spool of standard telecom fiber is used to build a long Sagnac loop. One light beam travels clockwise(CWS) and one counterclockwise(CCWS).

Sagnac loop: one light beam travels clockwise and the other one travels counterclockwise. After traveling along the Sagnac loop, the two beams interfere each other and the light goes partly back into the direction of the laser(one can say that is reflected) and partly into the direction opposite to the laser(one can say that is transmitted). A circulator is used to deviate the reflected light: if it goes inside the laser, it might damage the source. A circulator has three ports, as shown in fig.20: the input enters port 1 and goes out from port 2, then the reflected light enters from port 2 and exits from port 3. No light can exit the circulator from port 1. The mickey mouse PC (represented by three circles in fig.20) is used to control the interference of the Sagnac. The guiding fiber of the loop goes inside the three ears of the mickey mouse and here it can be twisted by moving the ears. When the fiber is twisted, a mechanical stress is induced in the fiber and consequently the polarization of the light changes. A polarization change means a different interference, thus by moving the mickey mouse one can control the intensity of the light that is reflected or transmitted: for instance one can choose to have all the light in transmission, or to have some light in transmission and some in reflection. The two detectors  $Dt$  and  $Dr$  are connected to an oscilloscope, where both the output signals(reflection and transmission) can be traced and recorded. In this part of the project, the voltage generator is connected to the electrodes that are inside the fiber, then the external field  $E_{ext}$  is generated between the two electrodes whose distance is  $d = 22.7\mu m$ .

## 4.2 Short electrical pulse

As first the light is modulated by short-pulse voltage, if the duration(width) of the pulse is shorter than the loop delay  $\Delta t$ , then a modulation of the light is seen at two instants for a single electrical pulse: if the poled fiber is placed as in fig.20, then the first modulation is given by the interference between the counterclockwise light(that has experienced the voltage pulse) and the clockwise light (that has not experienced the voltage pulse); after a time  $\Delta t$  there is the second modulation. Fig.21 shows the optical modulation given by an electrical pulse of frequency  $\nu = 1kHz$ , amplitude  $A=200V$  and width  $w = 100ns$ . The

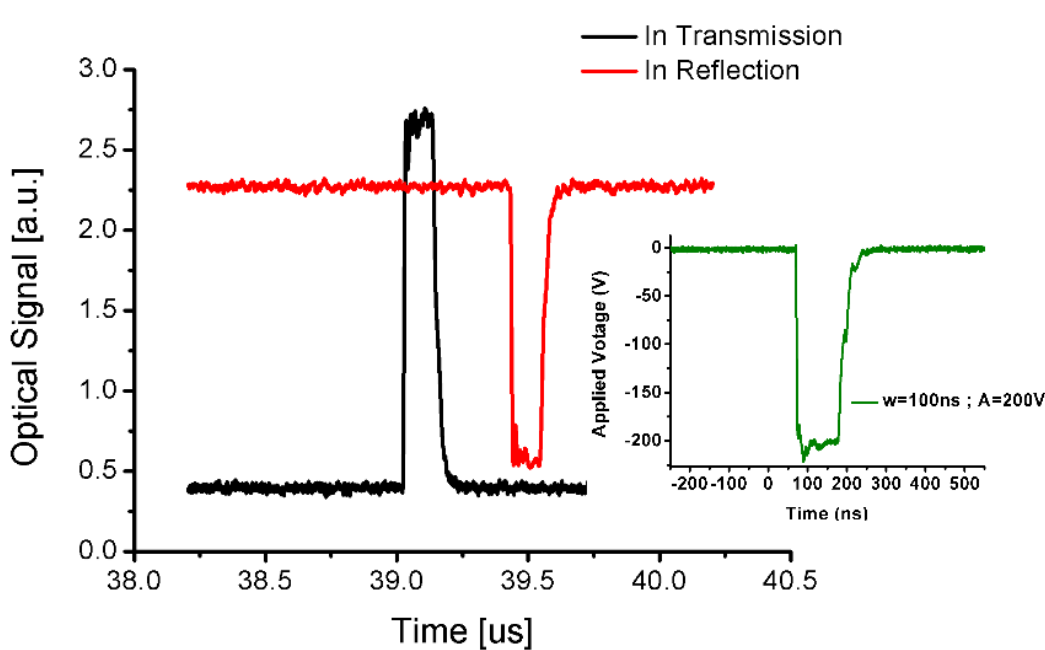


Figure 21: Optical signal in transmission(black) and in reflection(red) versus time. Applied voltage in the insert. The oscilloscope shows the output in milli-Volt(mV). However it is not known the mathematical relation between intensity and voltage of the detector, therefore the intensity of the optical signal is reported in arbitrary units (a.u.)

poled fiber is placed at the beginning of a loop of 7878m, that means a delay time of

$$\Delta t = \frac{7878m}{2 \cdot 10^8 \frac{m}{s}} = 39\mu s$$

Indeed, others two peaks(reflection and transmission) could be seen at  $39\mu s$  distance. The peaks in reflection and in transmission are complementary: if more light is transmitted, then less light is reflected since the total intensity does not change. When a setup for short-pulse voltage is arranged, it is important to remember that the applied voltage is transmitted through two electrodes that end in the glass of the fiber, without a resistive load: it is an open-circuit. When the voltage signal reaches the end of the electrode, it is reflected back and it can bounce back and forth between the electrode and the voltage generator [6]. The reflected pulses sum to each other, therefore the electrical pulse applied to the component results to be a pulse wider and with higher amplitude. To

overcome this problem, a resistance is connected to a second output channel of the pulse generator: when the electrical pulse is reflected, it goes back to the pulse generator and it is sent out from the second output channel, where it is dissipated by the resistance.

### 4.3 Malus law

Since the phase shift is linearly proportional to the applied voltage due to fiber poling, then the amplitude of the optical signal depends on the amplitude of the electrical pulse according to Malus law [7]:

$$I = I_{max} \cdot \left[ \sin\left(\frac{\pi V}{2 V_{\pi}}\right) \right]^2 \quad (6)$$

where  $I$  is the amplitude of the optical signal,  $V$  is the amplitude of the electrical pulse and  $I_{max}$  is the maximum amplitude seen when  $V = V_{\pi}$ . Measurements of the optical signals are read from the oscilloscope and plotted in fig.22, then a fitting is done by using eq.6. It results that  $V_{\pi} = 328/2 = 164V$ .

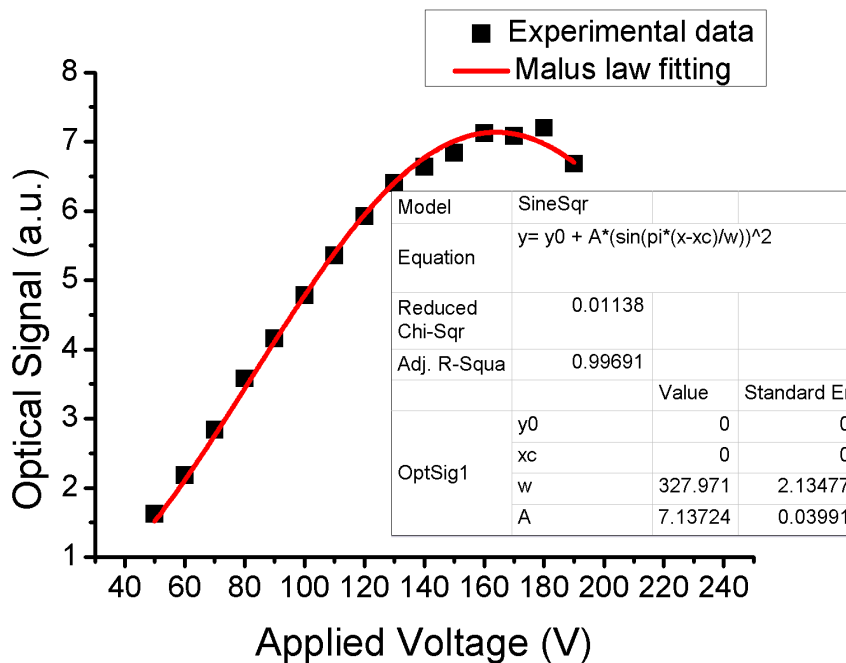


Figure 22: Optical signal vs. applied voltage(black square) follows the Malus law, as it is shown by the fitting(red line). The fitting parameter  $y_0$  and  $x_c$  are set to zero, in such a way to have a formula similar to eq.6. Here  $w$  is twice the  $V_{\pi}$  and  $A = I_{max}$ . The x-axis reports the amplitude of the applied electrical pulse.

#### 4.4 Sinusoidal voltage

The aim of the project is to develop a sensor to detect a sine wave voltage. Thus a generator of sinusoidal electrical signal is used and a voltage transformer is exploited to increase the amplitude of the applied voltage. Now the applied voltage is continuous and the interference does not occur anymore between one light beam that experiences a voltage and one light beam that does not. Both the clockwise and the counterclockwise light undergo a phase modulation before they interfere. For this reason, the relation between the delay given by the loop and the frequency of the applied signal becomes important. A delay of  $\Delta t = 39\mu s$  corresponds to a frequency of

$$\nu = \frac{1}{39\mu s} \sim 26kHz$$

Then, if the applied voltage has the same frequency of the loop delay, when the two light beams interfere, both of them have experienced the same voltage amplitude, thus the same phase shift. This means that there is no light modulation and the optical signals in reflection and transmission are the same as if no voltage is applied. In contrast, if the voltage has a frequency that is half the delay frequency, then there is a large modulation of the light. Fig.23 shows a schematic explanation.

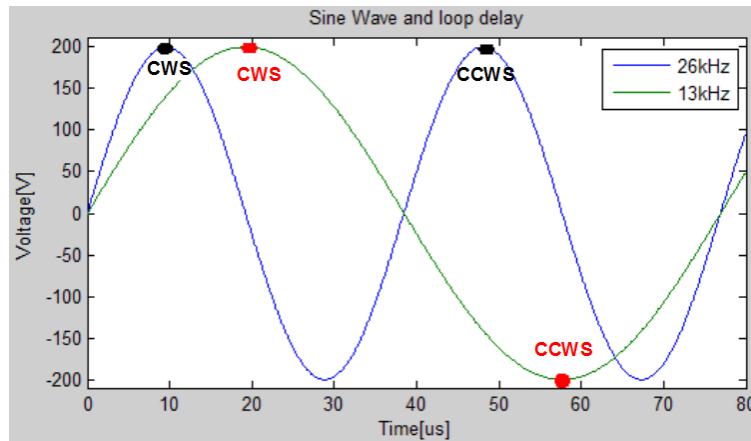


Figure 23: If the voltage signal has a frequency of 26kHz, the light beams (CWS and CCWS, black) undergo the same phase shift. If the frequency is half the loop delay, then CWS and CCWS light (red) undergo different phase shifts.

If the delay is much shorter than the period of the applied voltage, then the clockwise light experiences a voltage that is not much different from the voltage experienced by the counterclockwise light, fig.24: small voltage difference brings to small light modulation, that might be too small to be measured. Fig.25 and

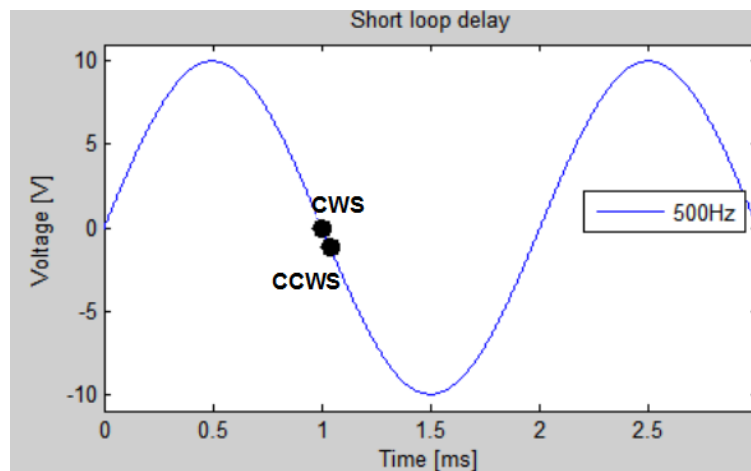


Figure 24: Applied voltage with  $\nu = 500\text{Hz}$  has a period much longer than a delay of  $\Delta t = 39\mu\text{s}$ , therefore the voltage difference between the two beams CWS and CCWS is very small and consequently the modulation is small and difficult to measure.

fig.26 show the data taken by applying sine wave voltages with frequencies of 13kHz and 26kHz. In fig.25 the voltage amplitude is high (as compared with  $V_\pi$ ) and a phase shift of  $\pi$  is achieved six times within one period of the applied voltage. In contrast, fig.26 shows a much lower modulation of the optical signal: if the frequency is exactly the frequency corresponding to the loop delay, then no modulation is expected.



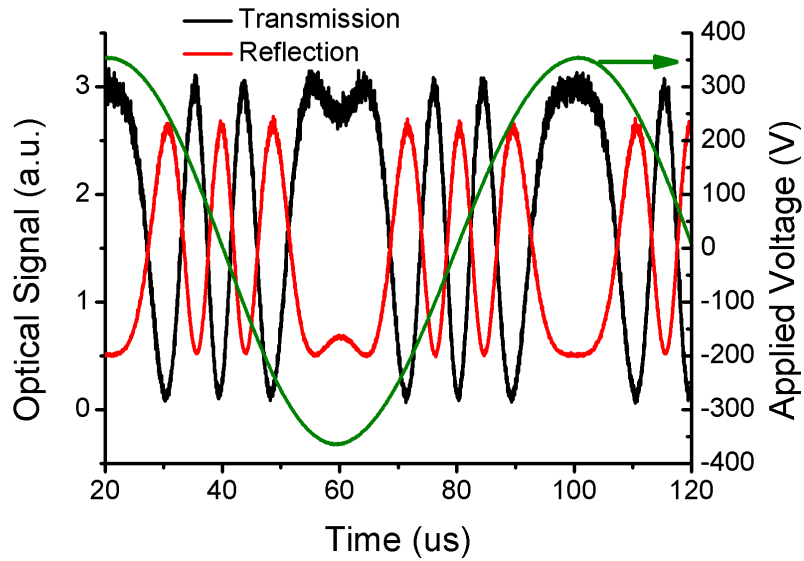


Figure 25: Transmitted(black) and reflected(red) light on the left scale and sine wave voltage(green) on the right scale. The amplitude peak to peak is  $V_{pp} = 720V$  and the frequency is  $\nu \sim 13kHz$ .

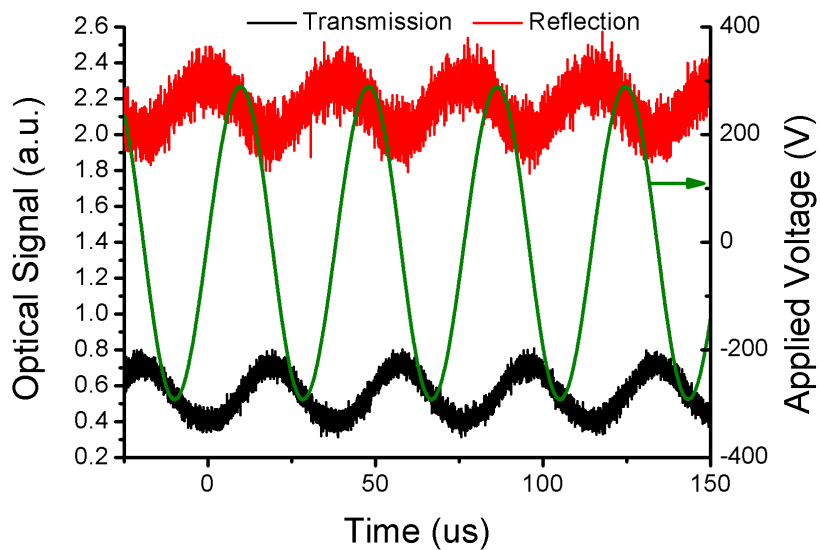


Figure 26: Transmitted(black) and reflected(red) light on the left scale and sine wave voltage(green) on the right scale.  $V_{pp} = 580V$  and  $\nu \sim 26kHz$ . Here the optical signal modulation is lower and there is more noise as compared with fig.25.

Afterwards, the voltage transformer is removed and the voltage generator is directly connected to the fiber electrodes. A lower voltage of  $V_{pp} = 20V$  is applied with a frequency of  $\nu \sim 13kHz$ . The amplitude is much lower than the value of  $V_{\pi}$ , then a  $\pi$ -shift is never reached and the modulation of light follows the sine wave voltage, fig.27. A comparison between fig.25 and fig.27

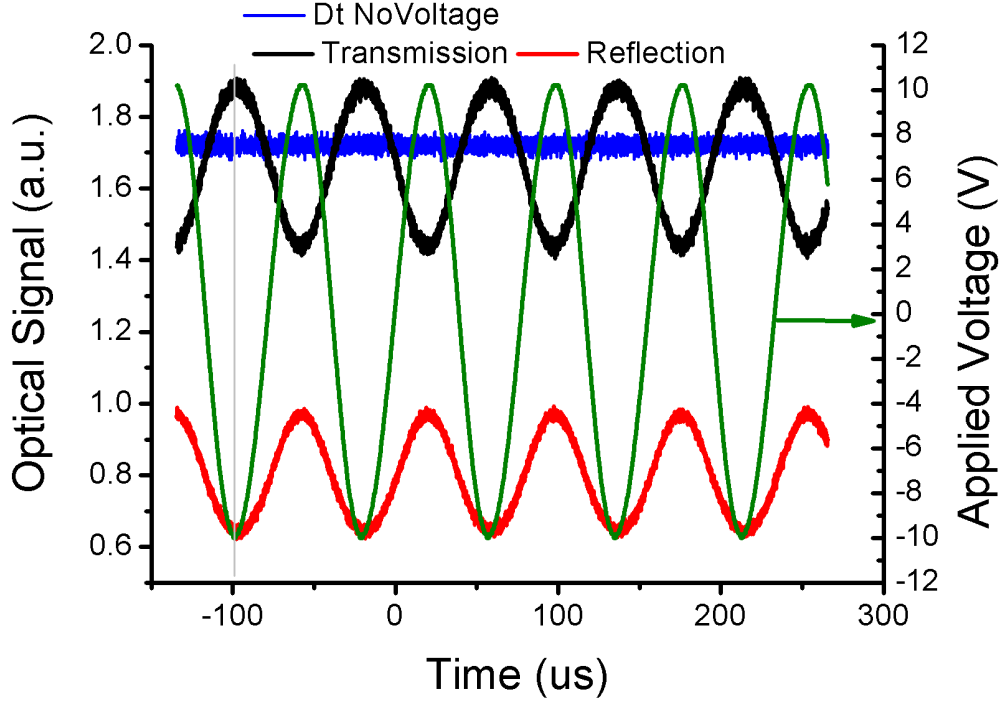


Figure 27:  $V_{pp} = 20V$  and  $\nu \sim 13kHz$ , the blue line shows the transmitted light (output read from detector Dt) before that the voltage is applied. Transmitted (black) and reflected (red) light modulations follow the period of the applied voltage (green).

shows how the light modulation (difference between maximum and minimum of the intensity: amplitude peak to peak) decreases as the voltage amplitude is reduced. Since the oscilloscope shows the output in mV, one can say that the light modulation goes from 3mV to 0.5mV when the amplitude of a sine wave voltage of  $\nu \sim 13kHz$  goes from  $V_{pp} = 720V$  to  $V_{pp} = 20V$ . This relation between applied voltage amplitude and light modulation can be exploited to calibrate the sensor.

#### 4.5 Intensity detected in a Sagnac

When the clockwise and the counterclockwise light interfere in a Sagnac, the intensity detected in transmission is described by:

$$I = A - B \cdot \cos(\Delta\Phi - k) \quad (7)$$

where  $k$ ,  $A$  and  $B$  are constant parameters and  $\Delta\Phi$  is the phase difference between CWS and CCWS light [8]. The parameter  $k$  refers to the light polarization and it explains why the detected intensity is seen to be unstable: the

Sagnac loop is built with a spool standard telecom fiber that does not maintain the polarization of the guided light, therefore the parameter  $k$  is not stable in time. This is one of the main reason of the instability of the output: if a measurement is taken and recorded, after few minutes a measurement of the same  $V_{app}$  will give a different result. According to eq.5 and eq.2, when the light goes through the poled fiber, it experiences a phase shift that depends linearly on  $E_{ext}$ . Since the electric field is proportional to the applied voltage  $E_{ext} = V_{app}/d$ , where  $d$  is the electrodes distance, then the phase difference  $\Delta\Phi$  is proportional to the difference between the voltage experienced by CCWS light at the time  $t$  and the voltage experienced by CWS light at the time  $t + \Delta t$  (or vice versa):

$$\Delta\Phi(t) \propto \left( V_{app}(t) - V_{app}(t - \Delta t) \right) \quad (8)$$

Since  $V_{app} = (V_{pp}/2) \cdot \sin(\omega t)$  and by using the definition of  $V_\pi$ , then eq.8 becomes:

$$\Delta\Phi(t) = \frac{\pi}{2V_\pi} V_{pp} \left( \sin(\omega t) - \sin(\omega(t - \Delta t)) \right) \quad (9)$$

By placing eq.9 into eq.7, one can see the function that describes the output in transmission of the Sagnac, that is the trace that one can see on the oscilloscope:

$$\begin{aligned} I(t) &= A - B \cdot \cos \left( \Delta\Phi(t) - k \right) = \\ &= A - B \cdot \cos \left( \frac{\pi}{2V_\pi} V_{pp} \left( \sin(\omega t) - \sin(\omega(t - \Delta t)) \right) - k \right) \end{aligned} \quad (10)$$

To make a sensor out of the Sagnac and the poled fiber, a relation has to be found between the amplitude of  $V_{app}$  and the output. Since the detected intensity looks like a sine wave, probably the best output parameter to measure is the intensity peak to peak  $I_{pp}$ , that is the difference between maximum and minimum intensity:

$$I_{pp} = I_{max} - I_{min} \quad (11)$$

By studying the maximum and minimum of eq.10(see Appendix A), one can see that there is a sort of borderline and two different working regime can be defined. One regime can be called "saturated regime" and here the voltage difference

$$\Delta V_{app}(t) = V_{app}(t) - V_{app}(t - \Delta t) \quad (12)$$

can reach values that are large enough to have  $\pi$ -shift in eq.10 and, then, switch from constructive to destructive interference. When this occurs, one can see multiple peaks(and troughs) within one period of  $V_{app}(t)$ , as in fig.25. From eq.10, it can be calculated that each of these peaks (or trough) is given by a value of  $\Delta V_{app}(t)$  that satisfies the following equation(see Appendix A for more details):

$$n = \frac{\Delta V_{app}(t)}{V_\pi} - \frac{k}{\pi} \quad (13)$$

where  $n$  is an integer. Therefore, there is a peak for  $n = 1$ , then a trough for  $n = 2$ , then a peak for  $n = 3$  and so on. The data shown in fig.25 are used to calculate the values of  $\Delta V_{app}$  that correspond to each switching of the interference: if the switching occurs at the time  $t$ , then  $\Delta V_{app}$  is given by the difference  $V_{app}(t) - V_{app}(t - \Delta t)$ . Fig.28 shows how the data are analyzed. The

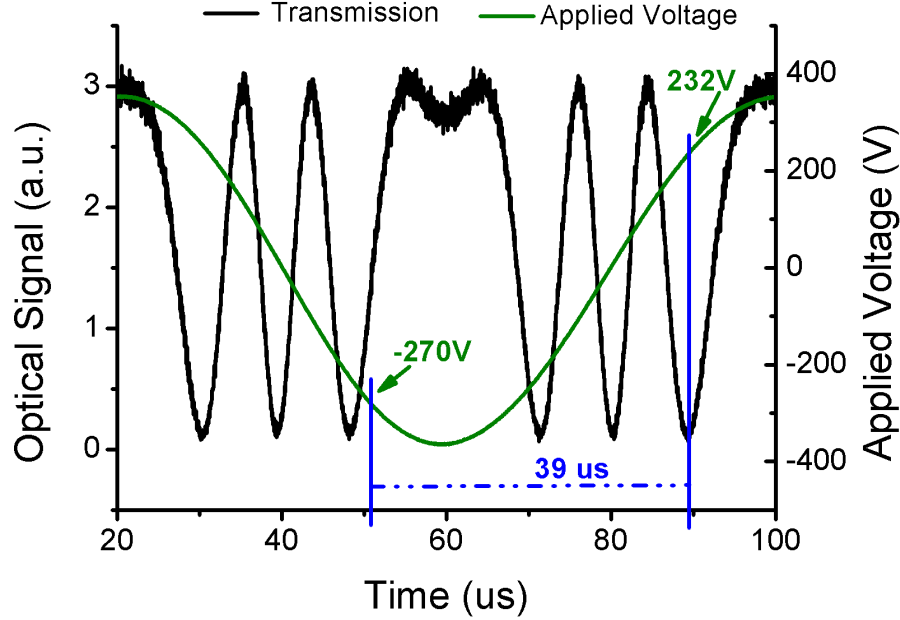


Figure 28: Zoom-in of fig.25. The loop delay is  $\Delta t = 39\mu s$ . The analyzed trough occurs at  $t = 89.3\mu s$ , then  $\Delta V_{app} = V_{app}(89.3\mu s) - V_{app}(50.3\mu s) = 232 + 270 = 502V$

calculated values are reported in table 1 and plotted in fig.29: according to eq.13, a linear plot is expected. The value of  $n = 0$  is given to the value of  $\Delta V_{app}$  closer to zero.

$t[\mu s]$	$V_{app}(t)[V]$	$t - 39[\mu s]$	$V_{app}(t - 39)[V]$	$\Delta V_{app}(t)[V]$	$n$
64.5	-336	25.5	327	-663	-3
71.5	-218	32.5	207	-425	-2
76.2	-102	37.2	84.6	-186.6	-1
80.3	9.78	41.3	-34.9	44.68	0
8.5	122	45.5	-155	277	1
89.3	232	50.3	-270	502	2

Table 1: The data are read within half period of the applied voltage, as shown in fig.28. Then the values of  $\Delta V_{app}$  are calculated and an integer number  $n$  is assigned to each peak and trough. Note that the difference between two consecutive  $\Delta V_{app}$  has a constant value of  $\sim 233V$ .

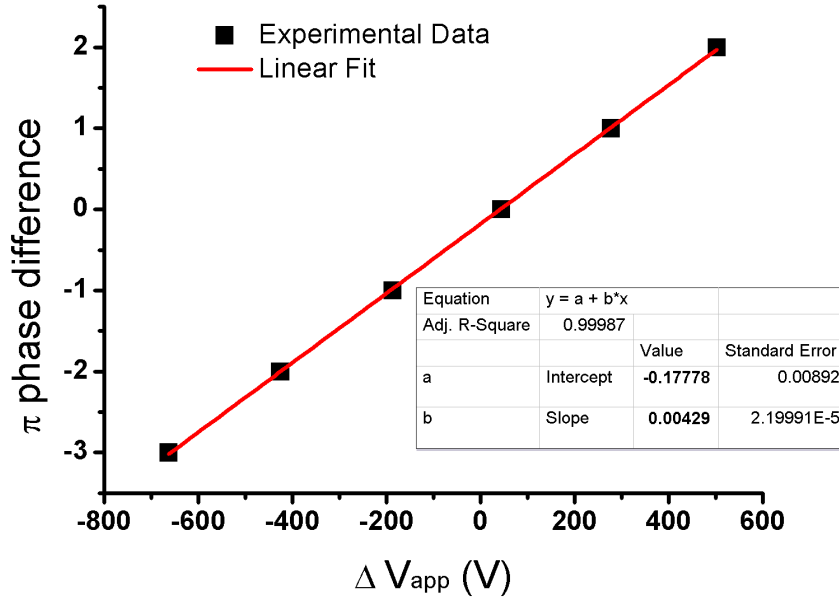


Figure 29: The data of table 1 are plotted and fitted by a linear function according to eq.13. The fit parameters are: slope  $b = 4.29 \cdot 10^{-3} V^{-1}$  and intercept  $a = -0.178$ .

The data of table 1 are read within a short time interval of  $\sim 65 \mu s$ . Then, one can assume that the parameter  $k$  of eq.7 is constant within this data range. Therefore, eq.13 and the fit parameters can be used to calculate the values of  $V_\pi$  and  $k$ . Here,  $V_\pi = 1/slope = 233V$  and  $k = -intercept \cdot \pi = 0.559rad = 32^\circ$ . By this analysis,  $V_\pi$  results to be much higher than in section 4.3 "Malus law", where eq.6 assumes that  $k$  is constant and equal to zero. This is likely due to the fact that in section 4.3 the parameter  $k$  is assumed to be constant. However the data are taken within a much longer time interval (the voltage is manually varied and the data are manually recorded, then few minutes are required), therefore the instability of  $k$  can not be neglected. To overcome this problem, when measurements are taken on a longer time interval, the PC mickey mouse needs to be used to adjust the light polarization and try to have the same value of  $k$  for all the measurements.

The first constructive-destructive intensity switching occurs for  $n = 0$  in eq.13, then the borderline between "saturated" and "not saturated" regime is given by the inequality,

$$\Delta V_{app}^{max} < \frac{k}{\pi} V_\pi \quad (14)$$

where  $\Delta V_{app}^{max}$  is the maximum value reached by  $\Delta V_{app}(t)$ . Eq.14 can be rewritten (see Appendix A for more details) as

$$V_{pp} < \frac{k V_\pi}{\pi \sin(\frac{\omega \Delta t}{2})} \quad (15)$$

Then, the PC mickey mouse can be used to control the value of  $k$ , thus the working regime. When the system is in the "not saturated" regime, the modulation of the optical signal is a sinusoid with the same frequency of  $V_{app}(t)$  and the optical amplitude  $I_{pp}$  is described by the function (see Appendix A for more details)

$$I_{pp} = 2B \sin(k) \sin\left(\frac{\pi V_{pp}}{V_{\pi}} \sin\left(\frac{\omega \Delta t}{2}\right)\right) \quad (16)$$

If eq.16 is seen as function of  $V_{pp}$ , then it can be approximated to a linear function when the following condition is satisfied:

$$V_{pp} \ll \frac{V_{\pi}}{\pi \sin\left(\frac{\omega \Delta t}{2}\right)} \quad (17)$$

Therefore,

$$I_{pp} = C V_{pp} \quad (18)$$

where  $C$  has a constant value of

$$C = 2B \sin(k) \frac{\pi}{V_{\pi}} \sin\left(\frac{\omega \Delta t}{2}\right) \quad (19)$$

This linear relation between input(applied voltage) and output (optical signal) makes the optical sensor to be very suitable for measuring sine wave voltages.

## 5 Sagnac interferometer and poled fiber for 50Hz electric field measurements

The developed sensor should work at  $50Hz$  and the idea is to exploit the electric field between the HV cable of a transmission line and the ground: approximately 15m distance. A voltage, for instance of  $75kV$ , over 15m means an electric field of

$$E_{ext} = \frac{75kV}{15m} = 5 \frac{kV}{m}$$

that corresponds to an applied voltage between the electrodes of

$$5 \frac{kV}{m} \cdot 20\mu m = 100mV$$

To measure this relatively weak electric field, improvements have to be made to the Sagnac interferometer setup. It is unrealistic to have a Sagnac loop that gives a delay of twice the voltage frequency:

$$\frac{1}{50Hz} = 20ms$$

then the loop delay should be of 10ms, that means loop length of

$$2 \cdot 10^8 \frac{m}{s} \cdot 10ms = 2000km$$

Such a long loop is unrealistic, therefore others features must be changed in the setup. A signal lower than 0.2mV can not be clearly seen on the oscilloscope, because it is too small. If the detector output is filtered by a lock-in amplifier, then a signal down to few  $\mu V$  can be detected.

A voltage of  $1MV$  is approximately the highest voltage that the sensor should capable to measure. It corresponds to an applied voltage between the electrodes of

$$\frac{1MV}{15m} \cdot 20\mu m = 1.33V$$

According to eq.17, at  $50Hz$  the condition of linearity is  $V_{pp} \ll 26V_{\pi}$ , then a value of  $V_{\pi}$  lower than  $233V$  would allow an enhancement of the output  $I_{pp}$  without breaking the condition of linear approximation. A lower  $V_{\pi}$  can be achieved by poling a longer fiber, for instance of 1m length. A further enhancement of  $I_{pp}$  is obtained by using a longer Sagnac loop: even if a 2000km loop is not possible, a length longer than 7878m would increase the sensor sensitivity.

## 5.1 Lock-in amplifier and longer loop

A lock-in amplifier is connected to the detector in transmission to filter the optical signal. Contrary to an oscilloscope, the lock-in amplifier does not show the trace of the light signal in time, but only a value that is proportionally related to the amplitude of the modulated light  $I_{pp}$ . Fig.30 shows the values of optical signal read from the lock-in for different voltage amplitude. As expected

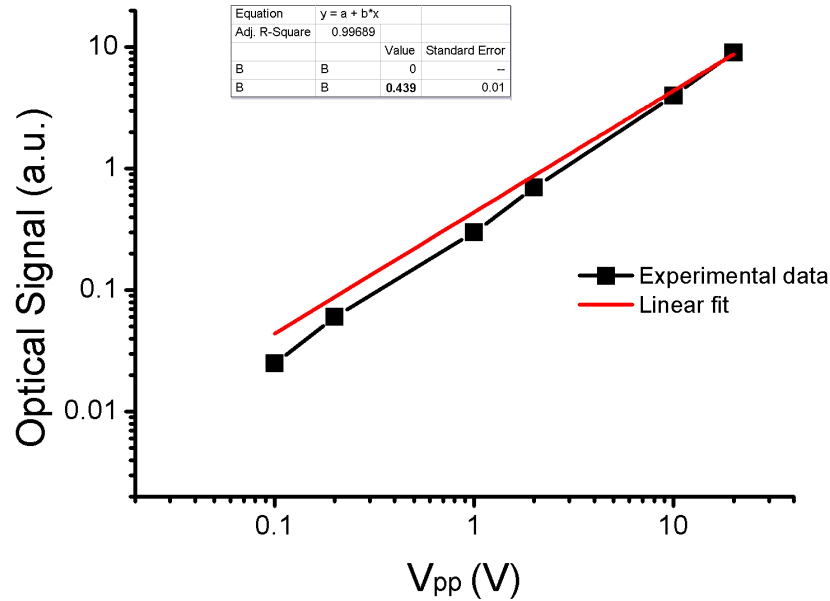


Figure 30: The output of the lock-in amplifier is plotted versus the amplitude of the applied voltage ( $V_{pp}$ ). Working frequency is 13kHz. Both the scales are logarithmic. The red line shows a linear fit where the intercept is forced to be zero, according to eq.18. The slope is  $0.44V^{-1}$ .

from eq.18, the data show a linear relation: an output signal of  $25\mu V$  is read from the lock-in amplifier when a sine wave voltage of  $V_{pp} = 100mV$  and  $\nu = 13kHz$  is applied. To read such a small signal, a time constant integration of 3s is set to average the signal and improve the signal/noise ratio. Then a longer loop of 25.3km is arranged with a delay of

$$\Delta t = \frac{25 \cdot 10^3 m}{2 \cdot 10^8 \frac{m}{s}} = 125 \mu s$$

that corresponds to nearly 8kHz. In table 2,  $V_{pp}$  is kept constant to 20V and the frequency is varied. At 50Hz a very high noise is observed and increasing the time constant integration does not improve the signal/noise ratio enough to take clear measurements. As expected from eq.16, low frequencies give weaker output, in addition the electronic devices show higher noise when they work at low frequency, according to Flicker noise. Moreover, most of the equipment in the lab works at 50Hz, therefore there is a lot of electromagnetic noise at 50Hz in the environment. Thin aluminum paper and a grounded metal box are used to isolate the poled fiber, but no significant improvement is achieved.



Voltage frequency	Optica signal [a.u.]
4kHz	14
2kHz	7.5
1kHz	2.5
100Hz	0.45
50Hz	0.24 - 0.29

Table 2:  $V_{pp} = 20V$ . When the frequency is 50Hz, the output oscillates within the range  $[0.24 \ 0.29]$ , even if a time constant integration of 10s is set.

Furthermore, the lock-in amplifier is powered by the standard electrical line that works at 50Hz: this generates an internal noise that makes even worse the signal/noise ratio. Because of all these reasons, the lock-in amplifier is very unstable at 50Hz and it is difficult to distinguish the optical signal from the noise.

To overcome the problem of bad signal/noise ratio at 50Hz, one solution is to make a poled fiber with low  $V_\pi$ . Then, the output signal will be higher and clearer distinguishable from the noise. In addition, a more powerful laser is tried out. The employed laser (emission power of  $-0.74dB$ ) is replaced with a more powerful tunable laser. Laser beams of 2mW and 5mW are shined into the fiber, but no significant improvement is observed.

## 5.2 Longer poled fiber

The poled fiber used so far is no longer than 30cm, then a sensing component of nearly 1m will significantly improve the sensitivity. However, it is very difficult to apply the experimental procedure of section 3.1 on a long fiber. First, during the "filling" process several gaps are most likely to occur and break the electrode continuity. Then, the processed fiber is moved into different working station(different labs room or working table) to complete all the steps and it is not easy to handle such a long and fragile fiber without breaking it.

A two-holes fiber is filled with 60cm continuous electrodes, after that gaps show up. Despite the gaps, the fiber is poled as described in section 3.1 and spliced to two connectors. The fabricated component has a loss of  $-7.50dB$ . The lock-in amplifier is connected to the oscilloscope, in this way the trace of the modulated optical signal can be seen. The wire connections of the fibers are used to apply a sine wave voltage across the internal electrodes. By applying a voltage of  $V_{pp} = 10V$  and varying the frequency, it is seen that the output has a maximum for  $\nu = 3.81kHz$  (that is closer to 4kHz) and a minimum for  $\nu \sim 8kHz$ , as expected. Measurements of the optical signal amplitude  $I_{pp}$  are taken by varying  $V_{pp}$  at a frequency of  $\nu = 3.81kHz$ , fig.31. The data follows eq.16 and  $V_\pi$  is calculated from the fit parameters. If  $\nu \sim 4kHz$ , then  $V_\pi = w$  where  $w$  is the fit parameter in fig.31: here,  $V_\pi = 410V$ .

Then, measurements for lower  $V_{pp}$  are performed and the data follow the linear approximation of eq.18: plot and fitting in fig.32. The plot in fig.32 is the continuation of the plot in fig.31 and the three lowest point (32, 20 and 10 V) are repeated in both the plotting.

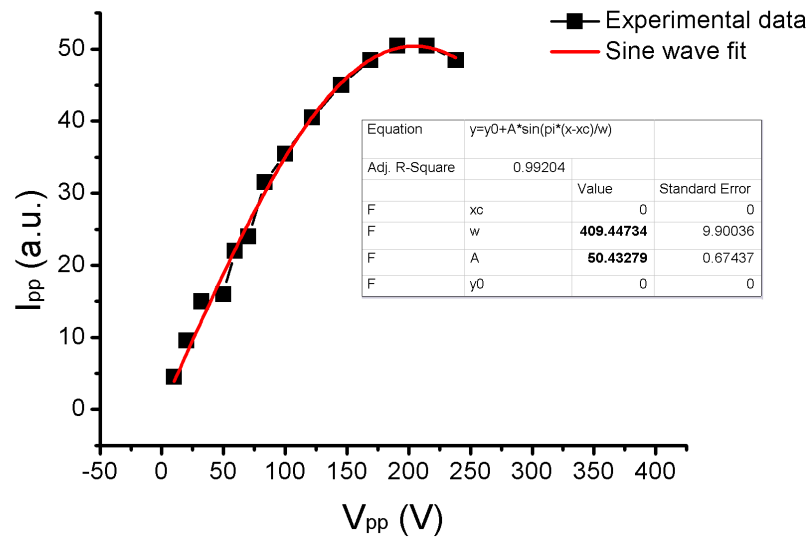


Figure 31: Frequency is set at  $\nu = 3.81kHz$ . According to eq.16, a sine function fits the data:  $y = A\sin(\pi/w \cdot x)$  where  $A = 50(a.u.)$  and  $w = 410V$ .

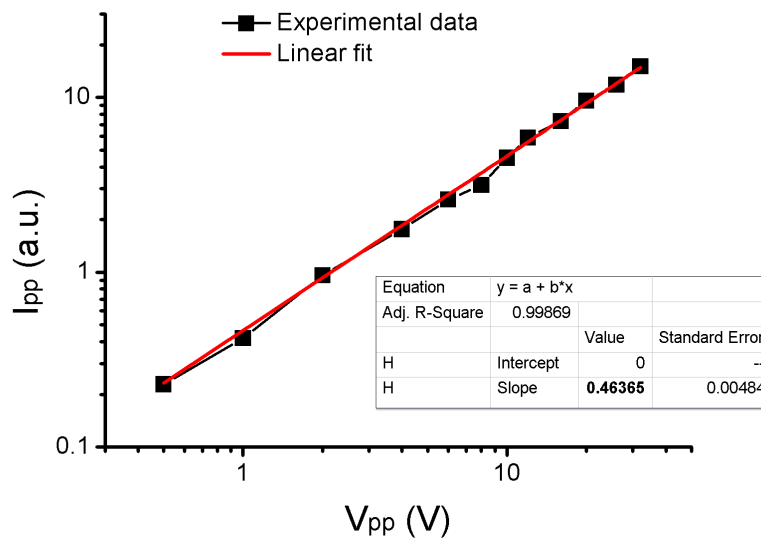


Figure 32: Frequency is set at  $\nu = 3.81kHz$ . According to eq.18, the intercept is set to zero and the slope is  $b = 0.46V^{-1}$ . The scales are both logarithmic to show better the lowest points.

Since the lock-in amplifier filters only the output signal at the reference frequency (voltage frequency), in this setup is not possible to see the saturated regime, in which the intensity peaks occur at different frequencies (see fig.25). When the saturate regime is reached, the result is that the lock-in filters a lower signal at the reference frequency. Then, the lock-in amplifier is temporarily disconnected and the oscilloscope reads directly the detector output. A voltage of  $V_{pp} = 380V$  and  $\nu = 3.73kHz$  is applied, the saturated regime is achieved, fig.33, and the method shown in fig.28 is repeated to calculate  $V_\pi$ . The applied

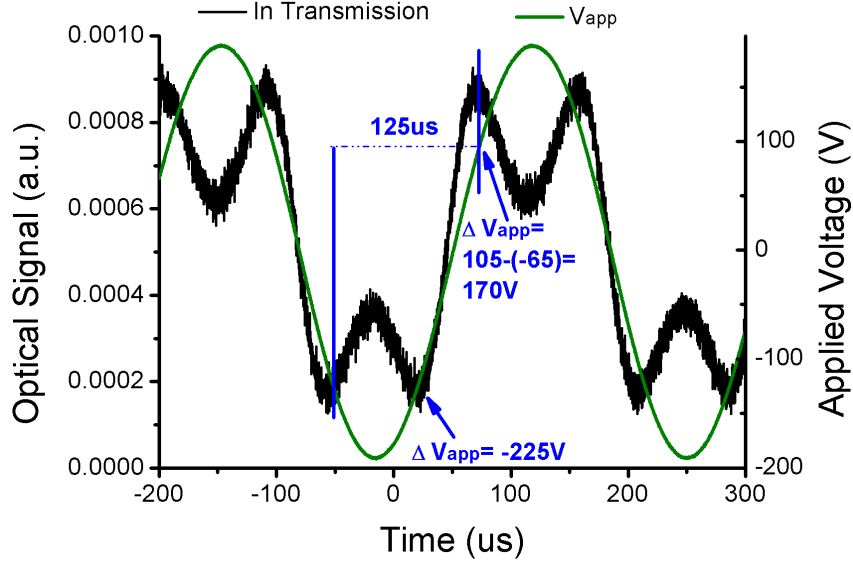


Figure 33: Applied voltage (green) of  $V_{pp} = 380V$  and  $\nu = 3.73kHz$ . There are two interference switches in half period. The two calculated value of  $\Delta V_{app}$  are shown and  $V_\pi = 170 - (-225) = 395V$ .

voltage difference  $\Delta V_{app}$  can be calculated only in two points, that correspond to  $n = -1$  and  $n = 0$ . The result of  $V_\pi = 170 + 225 = 395V$  is in agreement with the  $V_\pi$  value obtained by the fitting in fig.31. This component has a  $V_\pi$  that is almost twice higher than the component of section 4. After "filling", 60cm continuous electrodes were seen in the fiber, than a  $V_\pi$  smaller than 200V was expected. However, there were gaps inside the fibers and, since during poling the BiSn is liquid, these gaps can move. Therefore, during poling the gaps probably moved and broke the 60cm continuity of BiSn. Even if this component has a twice higher  $V_\pi$  than the previous one, the sensitivity in the linear region (eq.18) is the same:  $0.44V^{-1}$  (from fig.30) and  $0.46V^{-1}$ . This does not mean that  $V_\pi$  value is not relevant, but rather that parameters as  $k$  and  $B$  in eq.19 needs to be better controlled, for instance by making the system more stable.

Afterwards the lock-in amplifier is put back in the setup and the dependence of  $I_{pp}$  on the frequency is observed for a constant amplitude of  $V_{pp} = 32V$ , fig.34. At 50 Hz  $I_{pp}$  is two orders of magnitude lower than at 2.23 kHz.

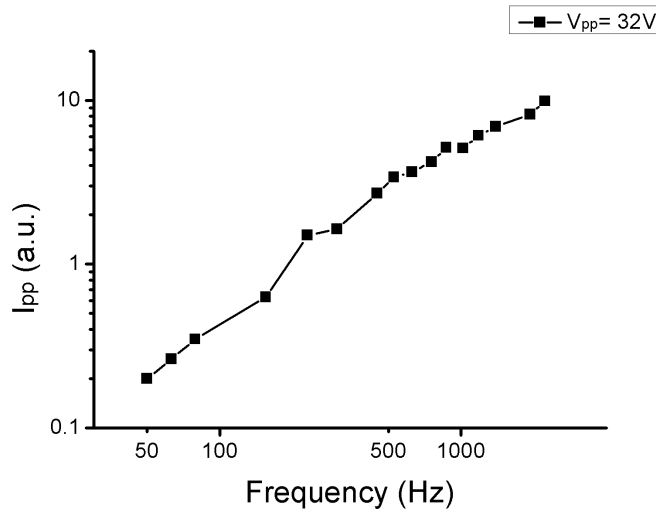


Figure 34:  $V_{pp}$  is kept constant to 32V. The frequency varies in a range [2.23 kHz 50 Hz]. The scale is logarithmic.

Fig.35 shows the output recorded on the oscilloscope for an applied voltage of  $V_{pp} = 28V$ . One can see a clear modulation of the light that follows the 50Hz applied voltage. A value of  $I_{pp} = 0.56a.u.$  can be read from the graph (black line). The electric field generated across the fiber is  $28/22.7\mu m = 1.23MV/m$ .

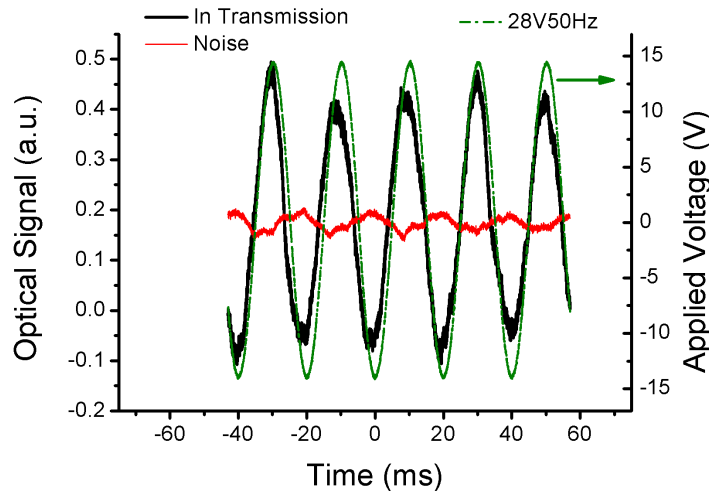


Figure 35:  $V_{pp} = 28V$  and  $\nu = 50Hz$  is applied (green). The red line shows the output when no voltage is applied. Therefore the output on the black line is definitely due to the light modulation given by the applied voltage. The scale of the oscilloscope is set on 1mV.

The employed voltage generator can not give 50Hz sinusoidal voltage higher than  $V_{pp} = 32V$ , then a voltage transformer working at 50Hz is directly connected to the AC transmission line and the oscilloscope trigger takes the AC line as reference. The voltage generator is still used to set the reference of the lock-in amplifier. Fig.36 shows plotting and linear fit of  $I_{pp}$  versus  $V_{pp}$  at 50Hz: a linearity is seen, as expected from eq.18. The functions describing the linear

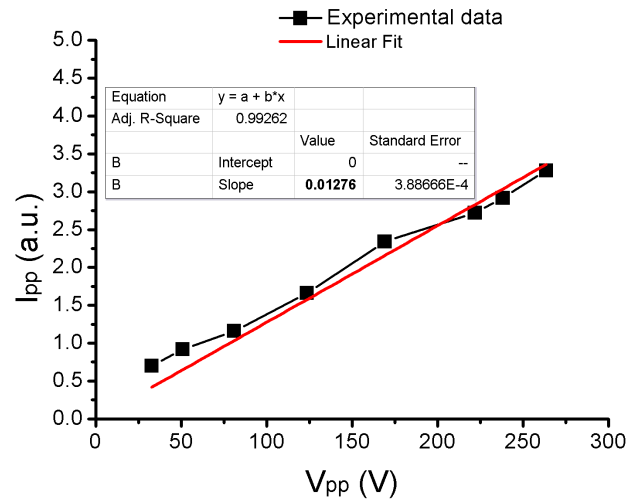


Figure 36: Values of  $I_{pp}$  are read from the oscilloscope for 50Hz applied voltages of different amplitudes. Linear fit has intercept equals to zero and slope of  $0.013V^{-1}$ .

region for this fiber component are:

$$I_{pp} = 0.46 V_{pp} \quad \text{at } 3.81kHz \quad (20)$$

and

$$I_{pp} = 0.013 V_{pp} \quad \text{at } 50Hz \quad (21)$$

At 50Hz the sensitivity is reduced by a factor of  $0.46/0.013 = 35$ .

## 6 Contactless detection of electric field

The electric field to measure is generated between the HV transmission line cable and the ground. An electrical connection with the internal electrodes is complicated, besides voltage breakdown would occur through the fiber if such a high voltages are applied between the  $20\mu\text{m}$  electrodes distance. For the application envisaged, a suitable sensor should work without the need of any connection. The sensor should be able to measure the electric field, just by being placed between the HV cable and the ground. For this reason an electrostatic parallel plates configuration is arranged and the poled fiber is placed in between without making any connection with the electrodes, fig.37.

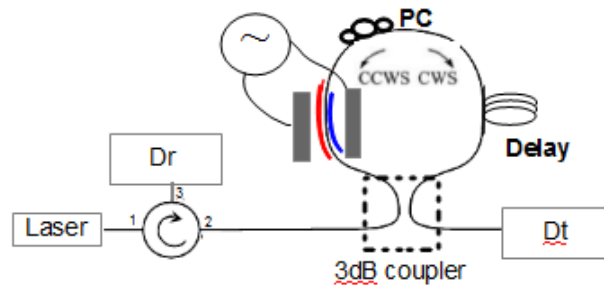


Figure 37: Sagnac interferometer:  $Dt$  and  $Dr$  are the detectors for transmitted and reflected light. Contrary to fig.20, a voltage generator is connected to two parallel plates and the component is sandwiched in between them.

### 6.1 Measurements of an electric field generated externally the fiber

A  $1.2\text{m}$  length fiber is filled with BiSn. However the process of "filling" did not work properly and only one of the two holes was filled with metal. Then, the fiber is coiled on the hot plate and poled by applying  $5\text{kV}$  to only one electrode ( $1.2\text{m}$  of continuous BiSn). After poling the component is spliced to two connectors and it is coiled on a small metallic plate, fig.38. The main

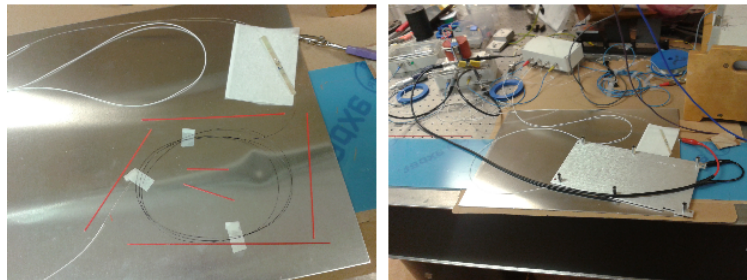


Figure 38: The component is fixed with tape and  $1\text{mm}$  thick multi-mode fibers (red) are used as spacer. Then a second metal plate is placed on the thick red fibers and crocodile clips are used to apply the potential.

issue of this configuration is that the component can not be aligned with the

applied electric field. To linearly modulate the phase of light according to eq.5, the recorded field  $E_{rec}$  has to be aligned with the external applied field  $E_{ext}$ , otherwise the linear effect will be reduced. Therefore, the component is stretched on a long and narrow metal plates as in fig.39. The fiber is gently

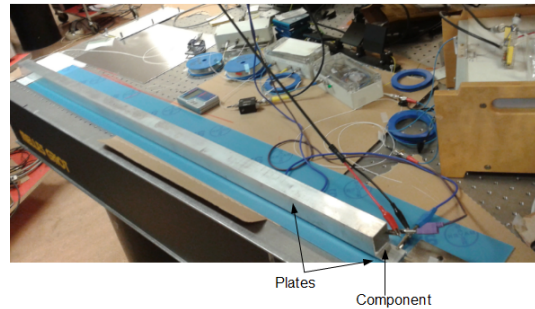


Figure 39: Multi-mode fibers is glued to the metal plate and the component is stretched. The plastic frame is not placed on the metal plates to avoid that the copper wire used for poling touches one of the parallel plates. Here, the component is sandwiched between two plates.

moved and turned, while the voltage potential is on; in this way the amplitude of the output is seen to vary. The explanation is that the alignment between  $E_{rec}$  and  $E_{ext}$  changes by moving the fiber. When the output is strong, the component is fixed with tape at the beginning and at the end of the plate. In the case of long parallel plates the output is seen to be much better compared with the case where the fiber is coiled on a small plate. Then the coating is removed by the multi-mode fiber to have thinner spacer, now 0.75mm. As unexpected result, this configuration shows a maximum of the optical signal at  $\nu = 1.5kHz$  and not only at  $\nu = 4kHz$ . Fig.40 show the result for an input of  $V_{pp} = 75mV$  and  $\nu = 1.5kHz$ , that corresponds to an electric field of  $75mV/0.75mm = 100V/m$ .

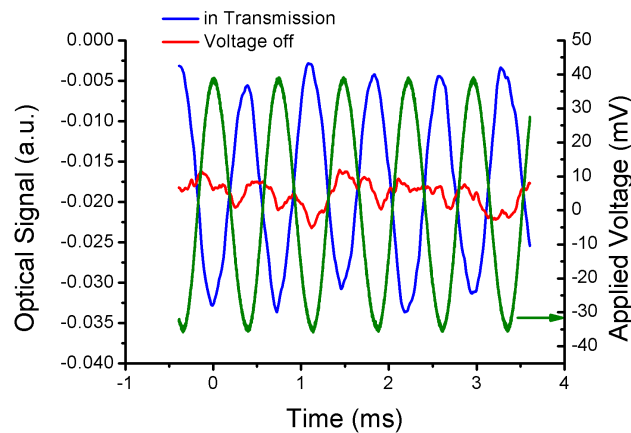


Figure 40: Green line is the applied voltage 75mV at 1.5kHz. The red line shows the detected intensity of light, when no voltage is applied.

Then a voltage of  $V_{pp} = 170V$  at 50Hz is applied to the plates. The electric field is  $170V/0.75mm = 227kV/m$ , fig.41. Measurements to lower voltage are

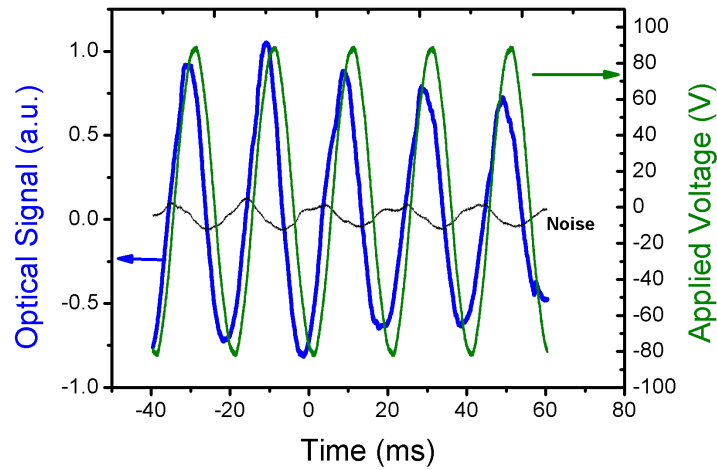


Figure 41: Green line is the applied voltage 170V at 50Hz. The black line shows the detected intensity of light, when no voltage is applied.

difficult to perform because of the noise. All the equipment in the lab works at 50Hz, moreover the power supply of the lock-in amplifier is the standard line, that is 50Hz. Therefore, there is both an external and an internal noise, that do not allow to use the lock-in with very low sensitivity to detect small signal. Fig.42 shows a modulation of light in three different cases:

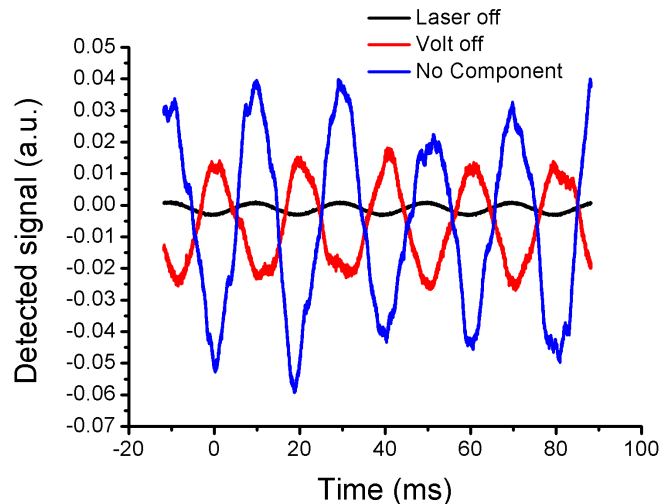


Figure 42: All the three lines should not have any modulation, however a modulation is seen in all the three cases.

- No voltage is applied.
- The component and parallel plates are removed from the Sagnac loop of fig.37



- the laser is off

In all the three cases there should not be any modulation, but an output at 50Hz is seen: noise. Even when no light is guided in the fiber, the lock-in shows a signal at 50Hz. If the metal plates and the component are removed from the Sagnac loop, the noise is almost the same that is detected as when the component is in the loop. Therefore, one can conclude that the noise is not originated by any "antenna" effect of the parallel plates.

Afterwards a third component is poled and the electrodes are removed by heating the fiber up to  $T = 160^{\circ}C$  and applying a pressure. A voltage of 100V at 1.33kHz is measured, fig.43.

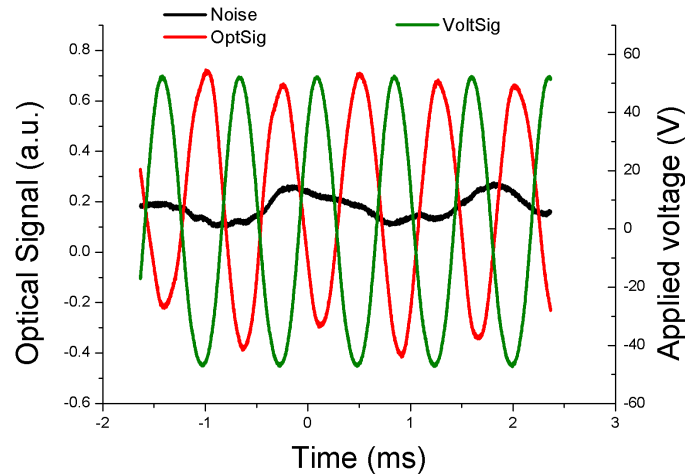


*Figure 43: A component with no metal inside is sandwiched between the parallel plates. A voltage of 1.33kHz and 100V is measured.*

## 6.2 Mobile plate

By placing a short plate on the component, fig.44, a scan of the alignment between the recorded field and externally applied field can be done. The short plate has a length of 12cm and is moved on different position of the fiber. A voltage of  $V_{pp} = 142V$  and  $\nu = 1.44kHz$  is applied on the short plate. For each position the optical amplitude  $I_{pp}$  is measured, table 3. By doing this

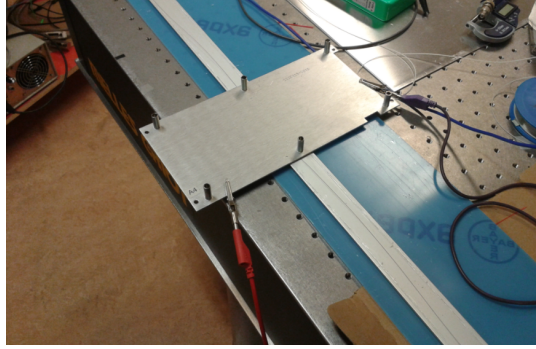


Figure 44: The component is scanned by moving a short plate connected to a voltage generator.

Optical Signal (a.u.)
0.180
0.100
0.336
0
0.080
0.215
1.05
0.190
0.056

Table 3: The modulation is measured in nine different point.  $E_{rec}$  is not aligned with  $E_{ext}$  along the whole fiber. The zero means that the two electric field go from a positive to negative (opposite direction) alignment.

procedure, the fiber can be rotated in such a way to maximize the output by aligning  $E_{rec}$  and  $E_{ext}$ .

## 7 Low fiber with a low coherence interferometer

A sensor for HV based on poled fiber is presented in [2] and [1]. A thermally poled fiber is inserted in a simple low coherence interferometer, as in fig.45 The

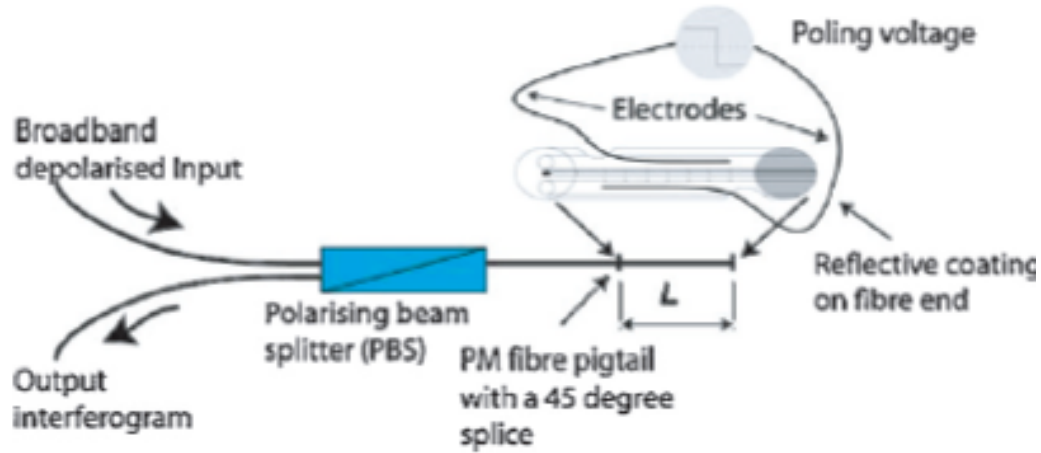


Figure 45: Experimental setup. Broadband light source is used [2].

sensing section consists of a Highly Birefringent (HiBi) fiber and a poled fiber, then the birefringence is not uniform along the length of the sensing section. The induced LEO effect gives a refractive index variation that is different for the two linear polarization modes

$$\Delta n(\lambda) = n_x(\lambda) - n_y(\lambda) \quad (22)$$

and it is linearly proportional to an electric field that cross the poled fiber core. Considering a voltage  $V$  proportional to the generated electric field:

$$\Delta n(\lambda) = kV \quad (23)$$

where  $k$  is the sensitivity constant. A broadband light source shines light into the interferometer and an AC voltage applied to the poled fiber generates a spectral modulation, or interferogram, whose phase is linearly proportional to the applied voltage.

The sensing section is placed in between two parallel plates, fig.46 shows the response of the sensor.

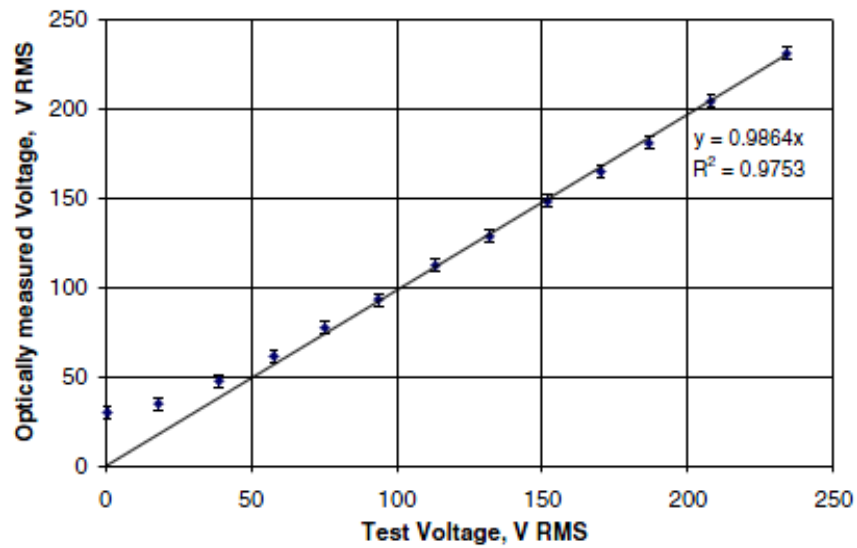


Figure 46: The response is linear. The voltage is in rms and below 50V rms the sensor detects high noise [1].

The plates distance is 0.5mm, then the sensitivity of this sensor is around  $50V/0.5mm = 100kVrms \sim 140kV/m$ , below this value the noise is too high. The Sagnac interferometer developed in this work has a sensitivity of  $227kV/m$ , but it has a big margin of improvement.

## 8 Conclusion

A 1.2m fiber is poled and inserted in a Sagnac interferometer for sensing applied voltage signal. Several measurements are taken at different frequencies and voltage amplitudes. Different methods are shown for characterizing the poled parameter as  $\chi_{eff}^{(2)}$  and  $V_\pi$ . A mathematical model is presented to describe the electro-optic response of the sensor and it is in agreement with the experimental results. A sinusoidal voltage of  $V_{pp} = 170V$  and  $\nu = 50Hz$  is applied across the fiber without making any contact with the electrodes inside the fiber. The generated electric field of  $227kV/m$  creates an optical modulation that was measured. Lower electric field could not be detected because of high noise. A much higher sensitivity is achieved for higher frequencies:  $100V/m$  is detected at 1.5kHz.

Instability of the system is seen: a measurement of the same applied voltage gives a different result if repeated after few minutes. This is due to the polarization state of light that is not maintained through the Sagnac loop, then the mickey mouse PC has to be used to maximize the signal before every measurement. When the parallel plate configuration is used, the main issue is to align the applied  $E_{ext}$  with the  $E_{rec}$ . A small movement of the poled fiber under the plate, gives a big change in the measured output. The issue of alignment might be solved during poling: if the fiber has only one electrode and it is placed on the hot plate in a way that the core is in between the electrode and the grounded plate. Then the fiber can be fixed to the hot grounded plate and the same plate used for poling can be used as grounded plate in the Sagnac interferometer, where a second plate is powered and placed on the top of the poled fiber to apply the  $E_{ext}$  to measure. A further improvement can be given by using maintaining polarization fiber to make the Sagnac loop. By controlling the polarization state, one can set the starting point (when no voltage is applied) with all the light in reflection and no light in transmission. From the mathematical point of view, this condition means to set  $k = 0$ . In this case the light modulation can not go below zero and instead of oscillating between  $I_{max}$  and  $I_{min}$ , the detected intensity will go from zero to  $I_{max}$ . This means that the optical signal has a frequency that is twice the frequency of the applied voltage, then the lock-in amplifier can be used to filter a 2nd harmonic, that is 100Hz. An optical signal with twice the frequency of the voltage was seen in the lab for higher frequencies. The bad point of this procedure is that the optical amplitude is reduced by a factor of 2, then one needs to evaluate if it is better to measure a bigger modulation at 50Hz or half modulation at 100Hz. A further and needed improvement is given by a component with a lower  $V_\pi$ , for instance a longer poled fiber. This would increase the output signal.

## A Appendix

The intensity detected in transmission is [8]:

$$I = A - B \cdot \cos(\Delta\Phi - k) \quad (24)$$

where  $A$  and  $B$  are parameters that depend on the transmission and reflection coefficients of the setup;  $k$  depends on the polarization state of the light.  $\Delta\Phi$  is the phase difference between the CWS and CCWS light:

$$\Delta\Phi(t) = \frac{\pi\Delta V_{app}(t)}{V_\pi} = \frac{\pi}{2V_\pi} V_{pp} \left( \sin(\omega t) \sin(\omega(t - \Delta t)) \right) \quad (25)$$

where the voltage difference between CWS and CCWS is

$$\Delta V_{app}(t) = V_{app}(t) - V_{app}(t - \Delta t) \quad (26)$$

Therefore eq.24 becomes

$$I(t) = A - B \cdot \cos \left( \frac{\pi}{2V_\pi} V_{pp} \left( \sin(\omega t) - \sin(\omega(t - \Delta t)) \right) - k \right) \quad (27)$$

The intensity peak to peak  $I_{pp}$  is the difference between maximum and minimum intensity:

$$I_{pp} = I_{max} - I_{min} \quad (28)$$

Eq.28 can be calculated by studying the maximum and minimum of eq.27, that means to calculate when the derivative is zero

$$\frac{dI}{dt} = 0 \quad (29)$$

The derivative of eq.27 is

$$\begin{aligned} \frac{dI}{dt} &= \quad (30) \\ &= -B \cdot \sin \left( \frac{\pi}{V_\pi} V_{pp} \left( \sin(\omega t) - \sin(\omega(t - \Delta t)) \right) - k \right) \cdot \\ &\quad \cdot \frac{\pi}{V_\pi} V_{pp} \left( \cos(\omega t) - \cos(\omega(t - \Delta t)) \right) = 0 \end{aligned}$$

There are two cases that satisfy this condition:

$$\sin \left( \frac{\pi}{V_\pi} V_{pp} \left( \sin(\omega t) - \sin(\omega(t - \Delta t)) \right) - k \right) = 0 \quad (31)$$

and

$$\cos(\omega t) - \cos(\omega(t - \Delta t)) = 0 \quad (32)$$

The first case is zero when

$$\frac{\pi}{V_{\pi}} V_{pp} \left( \sin(\omega t) - \sin(\omega(t - \Delta t)) \right) - k = n\pi \quad (33)$$

and since  $V_{app}(t) = \frac{V_{pp}}{2} \sin(\omega t)$ ,

$$\frac{\pi}{V_{\pi}} \Delta V_{app}(t) - k = n\pi \quad (34)$$

The maximum value of  $\Delta V_{app}(t)$  is given by  $\omega t = (\omega \Delta t)/2$  (it can be calculated from the derivative of  $\Delta V_{app}(t)$ ):

$$\Delta V_{app}^{max} = V_{pp} \sin\left(\frac{\omega \Delta t}{2}\right) \quad (35)$$

Therefore, eq.34 is never satisfied if the maximum voltage difference between CWS and CCWS is not enough. Then, this is the condition of the borderline between saturated and not-saturated region. The second case, eq.32, is satisfied when

$$\omega t = \frac{\omega \Delta t}{2} + n\pi \quad (36)$$

The second case represents the peaks (and troughs) of the modulated optical signal.  $n$  is an integer and for  $n = 0$  there is maximum, then for  $n = 1$  there is a minimum. For  $n = 0$ :

$$I_{max} = A - B \cos\left(\frac{\pi V_{pp}}{V_{\pi}} \sin\left(\frac{\omega \Delta t}{2}\right) - k\right) \quad (37)$$

For  $n = 1$ :

$$I_{min} = A - B \cos\left(\frac{\pi V_{pp}}{V_{\pi}} \sin\left(\frac{\pi + \omega \Delta t}{2}\right) - k\right) \quad (38)$$

Since  $\sin(\pi + x) = -\sin(x)$ , then the intensity peak to peak of the optical signal is

$$I_{pp} = I_{max} - I_{min} = -B \left( \cos\left(\frac{\pi V_{pp}}{V_{\pi}} \sin\left(\frac{\omega \Delta t}{2}\right) - k\right) - \cos\left(-\frac{\pi V_{pp}}{V_{\pi}} \sin\left(\frac{\omega \Delta t}{2}\right) - k\right) \right) \quad (39)$$

Since  $\cos(x - y) - \cos(x + y) = 2 \sin(x) \sin(y)$ , then

$$I_{pp} = 2B \sin(k) \sin\left(\frac{\pi V_{pp}}{V_{\pi}} \sin\left(\frac{\omega \Delta t}{2}\right)\right) \quad (40)$$

This formula describes the relation between input ( $V_{pp}$ ) and output ( $I_{pp}$ ).

## References

- [1] A.Michie, I.M.Bassett, J.H.Haywood, and J.Ingram, “Electric field and voltage sensing at 50hz using a thermally poled silica optical fibre,” *Meas. Sci. Technol.* 18, 2007.
- [2] A.Michie, I.Bassett, and J.Haywood, “Electric field and voltage sensing using thermally poled silica fibre with a simple low coherence interferometer,” *Institute of Physics Publishing, Meas. Sci. Technol.* 17, 2006.
- [3] R.Kashyap, F.C.Garcia, and L.Vogelaar, “Nonlinearity of the electro-optic effect in poled waveguides,” *OSA/BGPP*.
- [4] N. Myren, “Poled fiber devices,” *Doctoral Thesis, Department of Physics and Quantum Optics, Royal Institute of Technology, Stockholm*, 2005.
- [5] M. Fokine, L. E. Nilsson, A. Claesson, D. Berlemont, L. Kjellberg, L. Krummenacher, and W. Margulis, “Integrated fiber mach-zehnder interferometer for electro-optic switching,” *Optics Letters*, vol.27, No.18, 2002.
- [6] W.Margulis, “Dealing with ultrashort electrical pulses,” *Department of applied physics, KTH, Stockholm*.
- [7] O.Tarasenko and W.Margulis, “Electro-optical fiber modulation in a sagnac interferometer,” *Optics Letters*, vol.32, No.11, 2007.
- [8] G. T. Purves, “Sagnac interferometer: Theory & background, ch5,” *Thesis, Durham University*.